DOKUZ EYLÜL UNIVERSITY
GRADUATE SCHOOL OF NATURAL APPLIED SCIENCES

ADSORPTION OF MALACHITE GREEN ONTO CHITOSAN FROM AQUEOUS SOLUTION

by
Coşan ÖZVERİ

October, 2006
İZMİR

ADSORPTION OF MALACHITE GREEN ONTO CHITOSAN FROM AQUEOUS SOLUTION

A Thesis Submitted to the
Graduate School of Natural and Applied Sciences of Dokuz Eylül University
In Partial Fulfillment of
the Requirements for the Degree of Master of Science
in Chemistry

by
Coşan ÖZVERİ

October, 2006
İZMİR

M. Sc. THESIS EXAMINATION RESULT FROM

We have read the thesis entitled "**ADSORPTION OF MALACHITE GREEN ONTO CHITOSAN FROM AQUEOUS SOLUTION**" completed by **Coşan Özveri** under supervision of **Prof. Dr. Kadir YURDAKOÇ** and we certify that in our opinion it is fully adequate, in scope and in quality, as a thesis for the degree of Master of Science.

……..

Prof. Dr. Kadir YURDAKOÇ

Supervisor

…… **. ……**

Jury Member Jury Member

_____

Prof. Dr. Cahit HELVACI

Director

Graduate School of Natural and Applied Sciences

ACKNOWLEDGMENTS

The author is grateful to the supervisor of this thesis, Prof. Dr. Kadir YURDAKOÇ, for his valuable guide, help and advice, at all stages of this thesis study.

I would like also to thank to Res. Assist. Zehra Bekçi and Instructor Yoldaş Seki for their precious suggestions and discussions during the preparation of the thesis.

In addition, I wish to express my gratefulness to all friends for their continuous helpful encouragement and valuable supports.

Finally, I would like to thank my family for bringing me in this situation with their unique patience and supports.

Coşan ÖZVERİ

ADSORPTION OF MALACHITE GREEN ONTO CHITOSAN FROM AQUEOUS SOLUTION

ABSTRACT

The adsorption of malachite green (MG) onto chitosan was studied in a batch system as a function of temperatures, pH and contact time. Linear forms of Langmuir, Freundlich equations were applied to evaluate adsorption data. Langmuir adsorption isotherm gave better fit than Freundlich model based onto correlation coefficients values. By using Langmuir equation, maximum adsorption capacities (C_m) of chitosan were obtained as 93.55 mgL^{-1} at 30°C, 72.83 mgL^{-1}at 40°C and 82.17 mgL^{-1} at 50°C respectively. Freundlich K_f (adsorption capacity) values decreased from 28.38 mgL^{-1} at 30°C to 76.23 mgL^{-1} at 50°C. As a result, adsorption of malachite green increased by increasing temperature.

The adsorption removal of dye from aqueous solution was pH depended. The optimum adsorption condition at equilibrium was observed at pH=7.8 by plotting the amount of malachite green adsorbed by chitosan versus equilibrium pH. The interaction between cationic MG and the pair of electrons of nitrogen present in the structure of chitosan occurs. It is clear that the adsorption of dye onto Chitosan at basic pH values is quite high.

Several kinetic models including the pseudo-first-order-equation, pseudo-second-order equation and intraparticle diffusion model were applied to find out adsorption mechanism. The adsorption system obeys the pseudo-second-order kinetic model by taking into account of the correlation coefficients and the intraparticle diffusion is not the only rate-controlling step. Thermodynamic parameters; ΔH^o, ΔS^o, and ΔG^o were estimated and these parameters showed that occurred adsorption was endothermic. Activation energy value (E_a) is higher than 40 kJ mol^{-1}indicating chemical adsorption mechanisms. For all, it can be easily understood that chitosan can be used to remove malachite green from wastewater.

Keywords: adsorption, malachite green, chitosan, adsorption isotherms

MALAHİT YEŞİLİ'NİN SULU ÇÖZELTİDEN CHITOSAN ÜZERİNE ADSORPSİYONU

ÖZ

Malahit yeşilinin (MY) chitosan üzerine adsorpsiyonu kesikli sistemde sıcaklık, pH ve temas süresinin bir fonksiyonu olarak çalışılmıştır. Langmuir ve Freundlich adsorpsiyon izotermlerinin doğrusal denklemleri adsorpsiyon verilerini değerlendirmek için kullanılmıştır. Langmuir adsporpsiyon izotermi korelasyon katsayılarına göre, Freundlich modelinden daha iyi uyum göstermektedir. Langmuir eşitliğini kullanarak, chitosan için maksimum adsorpsiyon kapasiteleri (C_m) 30°C de 93.55 mgL^{-1}, 40°C de 72.83 mgL^{-1} ve 50°C de 82.17 mgL^{-1}olarak belirlenmiştir. Freundlich K_f (bağıl adsorpsiyon kapasitesi) değerleri ise 30°C için 28.38 mgL^{-1} ve 50°C için 76.23 mgL^{-1} olarak bulunmuştur. Sıcaklık arttıkça bağıl adsorpsiyon kapasitesi değerlerinin arttığı gözlenmiştir.

Yapılan deneyler sonucunda, sulu çözeltiden MY uzaklaştırılmasının pH' a bağlı olduğu bulunmuştur. Dengede optimum adsorpsiyon, denge pH'ına karşı chitosan tarafından adsorplanan malachite yeşil miktarını grafiğe geçirildiğinde pH=7,8 olarak gözlenmiştir. Chitosan'ın yapısında bulunan azottaki ortaklanmamış elektron çifti ile katyonik MY arasındaki etkileşim pH arttıkça adsorpsiyonun artmasını açıklamaktadır. Adsorpsiyon mekanizmasını bulmak için sahte birinci mertebeden tepkime kinetiğini, sahte ikinci mertebeden tepkime kinetiğini ve intraparticle difüzyon modelini içeren kinetik modeller uygulanmıştır. Adsorpsiyon sistemini korelasyon katsayılarını dikkate alarak değerlendirdiğimizde olay, sahte ikinci mertebeden tepkime kinetiğine uymaktadır. İntraparticle difüzyon modeli hızı kontrol eden tek basamak değildir. Termodinamik parametreler ΔH^o, ΔS^o, ve ΔG^o hesaplanmış olup parametreler gerçekleşen adsorpsiyonun ısı alan, yani endotermik olduğunu göstermektedir. Aktivasyon enerjisi (E_a) değeri, 40 $kJmol^{-1}$den daha yüksek olması gerçekleşen adsorpsiyonun kimyasal bir olay olduğunu göstermektedir. Tüm bunlardan, chitosanın atıksulardan malahit yeşilinin uzaklaştırılmasında kullanabileceği sonucu ortaya koymaktadır.

Anahtar sözcükler: adsorpsiyon, malahit yeşili, chitosan, adsorpsiyon izotermleri

CONTENTS

Page

THESIS EXAMINATION RESULT FROM……...ii
ACKNOWLEDGMENTS……...iii
ABSTRACT…….. iv
ÖZ…….v

CHAPTER ONE–INTRODUCTION…….……..1
1. The Adsorption – Desorption Process…….……1
1.1 Introduction to Adsorption Phenomena……1
1.2 Adsorption Processes……...…….……2
1.3 Factors Influencing Adsorption…...……4
1.3.1 Nature of the Adsorbent……...4
1.3.2 Nature of the Adsorbate…….. 4
1.3.2.1 Solubility of Adsorbate…….4
1.3.2.2 Molecular Sizes……4
1.3.2.3 Degree of Ionization…….5
1.3.2.4 pH……..5
1.3.2.5 Experimental Conditions……..5
1.4 Adsorption Isotherms…….……...…6
1.4.1 Langmuir Isotherm……6
1.4.2 Freundlich Isotherm…….……..8
1.4.3 BET Isotherm…….……9
1.4.4. Adsorption Enthalpy…….……....9
1.5 Adsorption Kinetics……..9
CHAPTERTWO–MALACHITE GREEN……..…12
2.1 Structure of Malachite Green…….....……12
2.2 Chromatic form of Malachite Green…….……..13
2.3 Toxicity - Effects on Humans…….…….13

CHAPTER THREE–CHITOSAN……..…15

3.1 Manufacture and Properties……...…….15

3.2 Usage…….....….……16

3.3 Biomedical Usage…….……...17

3.4 Claimed Benefits…….17

CHAPTER FOUR–MATERIAL AND METHOD……18

4.1 Synthesis of Chitosan Bead…….19

4.2 FTIR Study……..19

4.3 SEM Measurements……....19

4.4 Adsorption from Solution Experiments: Determination of Equilibrium Concentration of Malachite Green After Adsorption……..20

CHAPTER FIVE–RESULTS……..21

5.1 The Effect of Contact Time on Adsorption of Malachite Green onto Chitosan ……..…….……..22

5.2 Adsorption of Malachite Green onto Chitosan……..…..…..…24

5.3 Effect of pH on Adsorption of MG onto Chitosan……..29

5.4 Adsorption Kinetics…….……30

5.5 Thermodynamic Parameters of Adsorption…….39

5.6 SEM Analysis…….…….43

5.6.1 Surface Morphology……....44

5.7 FTIR Analysis…….49

CHAPTER SIX–CONCLUSION……51

6. Conclusion…….51

REFERENCES…….…….. 54

CHAPTER ONE

INTRODUCTION

1. The Adsorption – Desorption Process

1.1 Introduction to Adsorption Phenomena

Adsorption, the binding of molecules or particles to a surface, must be distinguished from absorption, the filling of pores in a solid. The binding to the surface is usually weak and reversible. Just about anything including the fluid that dissolves or suspends the material of interest is bound, but compounds with color and those that have taste or odor tend to bind strongly. Compounds that contain chromogenic groups (atomic arrangements that vibrate at frequencies in the visible spectrum) very often are strongly adsorbed on activated carbon. Decolorization can be wonderfully efficient by adsorption and with negligible loss of other material. (Rensselaer, 2006).

The most common industrial adsorbents are activated carbon, silica gel, and alumina, because they present enormous surface areas per unit weight. Activated carbon is produced by roasting organic material to decompose it to granules of carbon - coconut shell, wood, and bone are common sources. Silica gel is a matrix of hydrated silicon dioxide. Alumina is mined or precipitated aluminum oxide and hydroxide. Although activated carbon is a magnificent material for adsorption, its black color persists and adds a grey tinge if even trace amounts are left after treatment; however filter materials with fine pores remove carbon quite well. (Rensselaer, 2006).

A surface already heavily contaminated by adsorbates is not likely to have much capacity for additional binding. Freshly prepared activated carbon has a clean surface Charcoal made from roasting wood differs from activated carbon in that its surface is contaminated by other products, but further heating will drive off these compounds

to produce a surface with high adsorptive capacity. Although the carbon atoms and linked carbons are most important for adsorption, the mineral structure contributes to shape and to mechanical strength. Spent activated carbon is regenerated by roasting, but the thermal expansion and contraction eventually disintegrate the structure so some carbon is lost or oxidized (Rensselaer, 2006).

The use of solids for removing substances from either gaseous or liquid solutions has been widely used since biblical times. This process, known as adsorption, involves nothing more than the partitioning of substances from the gaseous or liquid phase on the surface of solid substances. From the early days of using bone char for decolorization of sugar solutions and the other foods, to the later implementation of activated carbon for removing nerve gases from the battlefield, to today's thousands of applications, the adsorption phenomenon has become a useful tool for purification and separation (Marczewski, 2002).

Adsorption phenomena are operative in most natural physical, biological, and chemical system, and adsorption operations employing solids such as activated carbon and synthetic resins are used widely in industrial applications and for purification of waters and waste waters (Marczewski, 2002).

1.2 Adsorption Processes

There is two type of adsorption, the first type is known as physisorption (physical adsorption) and the second one is called as chemisorption (chemical adsorption).

Adsorption in which the forces involved are intermolecular forces (van der Waals forces) of the same kind as those responsible for the imperfection of real gases and the condensation vapors, and which do not involve a significant change in the electronic orbital patterns of the species involved. The term van der Waals adsorption is synonymous with physical adsorption (IUPAC Compendium of Chemical Terminology 2nd Edition, 1997).

The only bonding is by weak van der Waals type forces. There is no significant redistribution of electron density in either the molecule or at the substrate surface.

A chemical bond, involving substantial rearrangement of electron density, is formed between the adsorbate and substrate. The nature of this bond may lie anywhere between the extremes of virtually complete ionic at complete covalent character. This is called as chemical adsorption (Blatt, et al, 1980, Hillier, 1995).

Table 1.1 Typical characteristics of adsorption process

Properties	**Chemisorption**	**Physisorption**
Binding force	Due to chemical forces or bonding, thus this process is also called as activated adsorption	Due to physical force of attraction, thus this process is also called as van der Waals adsorption
Saturation uptake	Single layer phenomena	Multilayer phenomena
Activation energy	May be involved	No activation energy involved
Temperature range (over which adsorption occurs)	Adsorption can take place even at higher temperature increases adsorption increases	Adsorption is appreciable at lower temperature below boiling of adsorbate. When temperature increases adsorption decreases
Nature of adsorption	Often dissociative may be irreversible	Non-dissociative Reversible
Crystallographic specify	Marked variation between crystal planes	Virtually independent of surface atomic geometry
Heat of adsorption	50-100 kcal/mole	1kcal/mole
Kinetic of adsorption	Very variable-often an activated process	FAST-since it is a non-activated process

The problem of distinguishing between chemisorption and physisorption is basically the same as that of distinguishing between chemical and physical interaction in general (Bekçi, 2005).

Changes in the electronic state may be detectable by suitable means (e.g. UV, infrared or microwave spectroscopy, electrical conductivity, magnetic susceptibility).

1.3 Factors Influencing Adsorption

1.3.1 Nature of the Adsorbent

The physicochemical nature of the adsorbent can have profound effects on both rate and capacity for adsorption. The rate of adsorption increases with increase in surface area of the adsorbent.

1.3.2 Nature of the Adsorbate

1.3.2.1 Solubility of Adsorbate

Adsorption of a solute is inversely proportional to its solubility in the solvent. The greater is the solubility, the stronger the solute-solvent bond and the small the extent of adsorption (Lundelius's rule).

On the other hand, the solubility of any organic compound in water decreases with increasing chain length, because the compound becomes more hydrocarbon-like as the number of carbon atoms becomes greater (Traube's rule).

1.3.2.2 Molecular Sizes

If the rate is controlled by intraparticle transport, the reaction generally will precede more rapidly the smaller the adsorbate molecule, within a given class of compound.

1.3.2.3 Degree of Ionization

As long as the compounds are structurally simple, adsorption is at minimum for the charged species and at a maximum for the neutral species. As compounds become more complex, the effect of ionization becomes of decreasing important.

Sorption mechanisms on clay surfaces have been studied for decades. One distinguishes between (i) inorganic cation exchange in the interlayer and on basal plane surfaces and (ii) specific pH-dependent sorption of cation and anions on clay edges. The edge sorption mechanism is a pH-dependent specific sorption on the clay edges. It has already been well established that the proton surface charge density on the clay edges depends on the physicochemical solution parameters (pH, ionic strength), which control the protonation state of the surface. In contrast, cation exchange on basal planes is related to the permanent negative charge generated in the clay structure created by isomorphic substitutions in the lattice. The density of exchange sites can be derived from the structural formula, and is compensated for by "exchangeable cations" which generally form outer sphere complexes with siloxane cavities (Tournassat, Greneche, Tisserand, & Charlet, 2004; Sposito, 1981; Sposito, 1984).

1.3.2.4 pH

Because hydrogen and hydroxide ions are adsorbed quite strongly, the adsorption of other ions is influence by the pH of the solution. In general, adsorption of typical organic pollutant from water is increased with decreasing pH. We should also take care of the ionization equilibrium of the adsorbate.

1.3.2.5 Experimental Conditions

Same of the conditions are temperature (Adsorption reaction are normally exothermic, thus the extent of adsorption generally increases with decreasing temperature), air flow velocity and relative humidity (Gereli, 2005).

1.4 Adsorption Isotherms

Adsorption isotherms describe the equilibrium conditions for an adsorbate onto surface of an adsorbent. Usually the amount of material adsorbed is some complex function of the concentration of adsorbate. Many theories and models have been developed to describe different types of isotherms. Some of them are Langmuir isotherm, Freundlich isotherms. B.E.T isotherms. (Seki, 2002).

1.4.1 Langmuir Isotherm

The simplest isotherm is based on the assumptions that every adsorption site is equivalent and that the ability of a particle to bind there is independent of whether or not nearby sites are accupied (Atkins P.W, 1990. Physical Chemistry, fourth edition, Oxford University Press).

The Langmuir equation is based on the following assumptions:

1. Adsorption of adsorbate molecules takes place at well-defined adsorption sites and each site can contain only one molecule.
2. The surface is homogenous; the energy of adsorption is equal for all adsorption sites.

Whenever a gas in contact with a solid there will be an equilibrium established between the molecules in the gas phase and the corresponding adsorbed species (molecules or atoms) which are bound to the surface of the solid.

As with all chemical equilibria, the position of equilibrium will depend upon a number of factors:

1. The relative stability of the adsorbed and gas phase species involved.
2. The temperature of the system (both the gas and surface).
3. The pressure of the gas above the surface.

In general, factor (2) and (3) exert opposite effects on the concentration of adsorbed species. We can say that the surface coverage may be increased by raising the gas pressure but will be reduced if the surface temperature is raised.

We may derive the Langmuir isotherm by treating the adsorption process as we would any other equilibrium process-expect in this case the equilibrium is between the gas phase molecules (M) , together with vacant sites, and the species adsorbed on the surface. Thus, for a non dissociative (molecular) adsorption process we consider the adsorption to be represented by the following chemical equation:

$$S\text{-}* + M_{(g)} \rightleftharpoons S-M$$

In writing these equations we are making an inherent assumption that is fixed number of localized surface sites present on the surface.

We may now define an equilibrium constant (K) in terms of the concentrations of 'reactants' and 'products',

$$K = \frac{[S-M]}{[S-*][M]}$$

We may also note that:

- [S-M] is proportional to the surface coverage of adsorbed molecules, i.e proportional to θ,
- [S - *] is proportional to the number of vacant sites, i.e. proportional to (1-θ),
- [M] is proportional to the pressure of gas, P.

Hence, it is also possible to define another equilibrium constant, b, as given below:

$$b = \frac{\theta}{(1-\theta)P}$$

Rearrangement then gives the following expression for the surface coverage

$$\theta = \frac{bP}{1+bP}$$

This is the usual form of expressing the Langmuir Isotherm.

As with all chemical reactions, the equilibrium constant and b are both temperature dependent and related to the Gibbs free energy and hence to the enthalpy change for the process.

1.4.2 Freundlich Isotherm

The Empirical Freundlich expression is an exponential equation and therefore, assumes that as the adsorbate concentration increases so too does the concentration of adsorbate on the adsorbent surface. Theoretically, using this expression, an infinite amount of adsorption can occur (Freundlich, 1906).

Freundlich equation is based on monolayer adsorption by the adsorbent with a heterogeneous energy distribution of active sites (Aksu & Kabasakal, 2004).

$$C_s = K_f C_e^{nf}$$

In this equation K_f and n_f are the Freundlich constants characteristic on the system. K_f and n_f are indicators of adsorption capacity and heterogeneity factor, respectively.

The Freundlich equations aggress well with the Langmuir equation; it does not reduce to the linear isotherm at low surface and provides no information on the monolayer adsorption capacity (Allen et al, 2003).

To determine the constants K_f and n_f , the linear form of the equations shown below may used to produce a graph of $\ln C_s$ against $\ln C_e$ (Allen et al , 2003).

$\ln C_s = \ln K_f + n_f \ln C_e$

From slope and intercept of the graph, we can calculate K_f and n_f values.

1.4.3 BET Isotherm

Derivation of the Langmuir isotherm expression was based on the idea of coverage of the surface with single layers of adsorbent. Isotherms curves for adsorption rather than flatten out after initial stage of adsorption suggest a secondary adsorption stage. S. Brunauer, P.H Emmett, and E.Teller have worked out a description of this process, and expression for the corresponding adsorption isotherm known as the BET isotherm (G. M. Barrow, 1996).

1.4.4. Adsorption Enthalpy

Since Adsorption is an exothermic process, energy is liberated, so that enthalpy is always negative. Adsorption constants are equilibrium constants; therefore they obey van't Hoff's equation,

$$\left(\frac{\partial \ln K}{\partial \frac{1}{T}} \right)_{\theta} = - \frac{\Delta H}{R}$$

As can be seen in the formula, the variation of K must be isosteric, that is, at constant coverage.

1.5 Adsorption Kinetics

The rate of adsorption, R_{ads}, of a molecule onto a surface can be expressed in the same manner as any kinetic expression: i.e.

$R_{ads} = k\, C^x$

where,

x - kinetic order,

k - rate constant,

C - gas phase concentration.

If the rate constant in either of the above expressions is expressed in an Arrhenius form then we obtain kinetic equations of the form:

$R_{ads}=AC^{x}e^{-E/RT}$

where, E_a is the activation energy for adsorption, A is the pre-exponential (frequency) factor. The rate of adsorption is governed by

1. The rate of arrival of molecules at the surface.

2. The proportion of incident molecules which undergo adsorption.

We can express the rate of adsorption (per unit area of surface) as a product of the incident molecular flux, F and the sticking probability, S.

$R_{ads} = S\,F$

$S = f(\theta)e^{-E_a/RT}$ and $F = \dfrac{P}{\sqrt{2\pi\, mkT}}$ Hertz-Knudsen equation

where, E_a is the activation energy,

f (θ) is some, as yet undetermined, function of the existing surface coverage of adsorbed species,

P is gas pressure (Pa),

m is mass of one molecule (kg),

T is temperature (K).

Combining the equations for S and F yields the following expression for the rate of adsorption:

$R= [f(\theta)\, P / 2\pi\, mkT)^{1/2}] \exp(-E_a / RT)$

Note:

1. It should be recognized that the activation energy for adsorption may itself be dependent upon the surface coverage, i.e. $E_a = E(\theta)$.

2. If it is further assumed that the sticking probability is directly proportional to the concentration of vacant surface sites (which would be a reasonable first assumption for non-dissociative adsorption) then $f(\theta) = (1-\theta)$; where, in this instance, (θ) is the fraction of sites which are occupied (i.e. the Langmuir definition of surface coverage).

It is known that there are three consecutive steps in the adsorption of substances by a porous adsorbent. These steps can be expressed as follows 1. Film diffusion step (boundary layer).

CHAPTER TWO
MALACHITE GREEN

2.1 Structure of Malachite Green

Chemical structure of the malachite green can be seen in Figure 2.1.

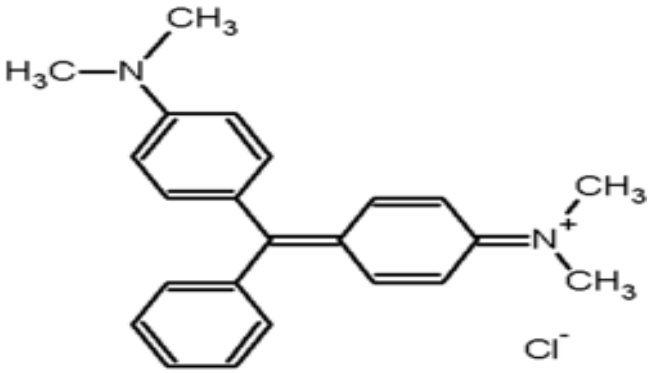


Figure 2.1. Structure chromatic form of malachite green green with chlorine salt

Malachite green, (IUPAC name: 4-[(4-dimethylaminophenyl)-phenyl-methyl]-N,Ndimethyl-aniline) is a toxic chemical primarily designed to be a dye and has foundextensive use all over the world in the fish farming industry as a fungicide, ectoparasiticide and disinfectant in fish and fish eggs. However, MG is highly cytotoxic to mammalian cells and acts as a tumor enhancing agent. This dye may enter the food chain and could possibly cause carcinogenic, mutagenic and taratogenic effects on humans.

Three forms of malachite green can be seen below in Figure 2.2.

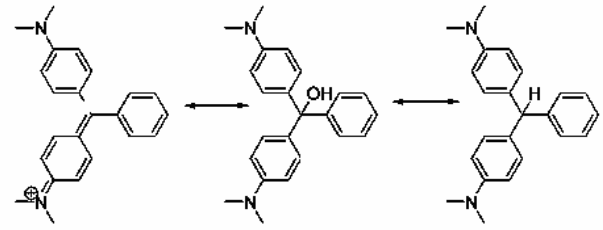


Figure 2.2 Structures of malachite green and related compounds

The first form in Figure 2.2 is called the Carbinol form, which is important because it spreads across cell membranes faster. When it is inside the cell, it is then metabolized into a form called Leuco Malachite Green. This form is known by researchers to be toxic in addition to the fact that it is retained in the body for a longer period than the chromatic form of malachite green. (http://en.wikipedia.org/wiki/Malachite_green).

2.2 Chromatic form of Malachite Green

MG is generally used for the dyeing of wool, silk, leather, cotton, jute, etc. and is also found to be especially active against the fungus Saprolegnia, which infects fish eggs in commercial aquaculture.

Malachite green is known to be highly toxic to certain freshwater fish such as tetras, catfish and shark catfish.

Malachite green is used as a biological stain for microscopic analysis of cell and tissue samples. Malachite green can be used as a gain medium in dye lasers.

Lecuco malachite green (LMG) is used as a detection method for latent blood in criminalistics.

2.3 Toxicity - Effects on Humans

Malachite green and its major metabolite, leuco malachite green has been reported to have mutagenic and carcinogenic effects.

Culp SJ in her recent article published in Mutation Research mentions that rats fed malachite green experience “a dose-related increase in liver DNA adducts” along with lung adenomas. Leucomalachite green causes an “increase in the number and severity of changes”. As Leucomalachite green is the primary metabolite of

malachite green and is retained in fish muscle much longer, most intake of malachite green would be in the leuco form and it could be concluded that a malachite green caused carcinogenic symptoms but a direct link between malachite green and liver tumour could not be proved (http://en.wikipedia.org/wiki/Malachite_green).

CHAPTER THREE

CHITOSAN

3.1 Manufacture and Properties

Most industries use dyes and pigments to color their products, which include textile, tannery, food, paper and pulp, printing, carpet and mineral processing industries. Perhaps these are the serious polluters of our environment as far as color pollution is concerned. Discharge of dye effluents into the natural streams may be toxic to the aquatic lives. Color affects the nature of water and inhibits the sunlight penetration into the stream and reduces photosynthetic activity. Some of the dyes are carcinogenic and mutogenic (K. Vasanth Kumar, V. Ramamurthi & S. Sivanesan, 2005).

Color is a visible pollutant and the presence of even very minute amount of coloring substance makes it undesirable due to its appearance. Removal of color from dye bearing wastewaters is a complex problem because of difficulty in treating such wastewaters by conventional treatment methods. Te most commonly used method of color removal is biological oxidation and chemical precipitation. However, these processes are effective and economic only in the case where the solute concentration is relatively high. Currently sorption process is proved to be an effective alternate for the treatment of dye waste waters. Activated carbon is the most commonly used adsorbent for the treatment of dye bearing wastewaters. However, this process is proved to be uneconomic due to the high cost of activated carbon and also the additional cost involved in regeneration. This process becomes economic, if the sorbent inexpensive and does not require any expensive pretreatment. Thus there is a continuous search for alternate low-cost adsorbent material (for example chitosan) to replace high cost activated carbon for water and wastewaters treatment (K. Vasanth Kumar, V. Ramamurthi & S. Sivanesan, 2005).

Chitosan is a copolymer consisting of β-(1-4)-2- acetamido-D-glucose) and β-(1-4)-2-amino-D-glucose units with the latter changing usually from 60 to 90 % (degree of deacetylation). Chitosan is prepared from chitin by deacetylation in the presence of alkali.

When its DA (degree of N- acetylation) is lower than 50%, the chitin becomes soluble in aqueous acidic solution and is named chitosan. Up to the present time only a few cationic polymers exist and chitosan may be used as a flocculation and chelating polymer (Pham le Dung, Michel Milas, Marguerite Rinaudo & Jacques Desbrieres, 1994).

3.2 Usage

Chitosan has been extensively over a wide range of applications such as prevention of water pollution by chelating heavy metals or radioactive isotopes membrane separation in medicine and biotechnology, and in the food-related areas either as food packaging material because of its antimicrobial action or as diatery fiber and potential medicine against hypertension thanks to its scavenging action for chloride ions (M. Mucha, S. Ludwiczak, & M. Kawinska, 2005).

High-molecular polysaccharides including chitosan can adsorb water easily, mainly by hydrogen bonds which are formed with hydroxyl and amide groups present in its structure (M. Mucha, S. Ludwiczak &M. Kawinska, 2005).

Chitosan can also be used in water processing engineering as a part of a filtration process. Chitosan causes the fine sediment particles to bind together and is subsequently removed with the sediment during sand filtration. Chitosan also removes phosphorous, heavy minerals, and oils from the water. Chitosan is an important additive in the filtration process (http://en.wikipedia.org/wiki/Chitosan).

Chitosan is also useful in other filtration situations, where one may need to remove suspended particles from a liquid. Chitosan, in combination with bentonite,

gelatin, silica gel, isinglass, or other fining agents is used to clarify wine, mead, and beer. Chitosan combined with colloidal silica is becoming a popular fining agent for

white wines, because chitosan does not require acidic tannins (found primarily in red wines) to flocculate with.

3.3 Biomedical Usage

Chitosan's properties allow it to rapidly clot blood, and have recently gained approval in the USA for use in bandages. The bandages include a layer of carefully produced chitosan that, when applied to a wound, causes rapid clotting, stopping the bleeding. Chitosan is hypoallergenic, and has natural anti-bacterial properties, further supporting its use in field bandages.

3.4 Claimed Benefits

Chitosan affects fat in the stomach before it has a chance to become metabolized. It dissolves in the stomach and converts to a gel which "traps" fat, thereby preventing its absorption and subsequent storage. Chitosan renders the fat useless to the body. Technically, it creates a "grease ball" out of excess fat which is then too large to be absorbed. Both the chitosan and the fat are excreted in the stool (www.vanderbilt.edu/AnS/psychology/health_psychology/chitosan.htm).

Besides absorbing fat to promote weight loss, chitosan also inhibits bad cholesterol and boosts good cholesterol. It also promotes healing of ulcers and lesions. It has anti-bacterial and anti-candida action. Chitosan acts as an antacid. Chitosan may help to control high blood pressure. It may treat and prevent irritable bowel syndrome. Chitosan helps to prevent constipation. It is a calcium enhancer and bone strengthener. Chitosan also reduces blood levels of uric acid (which causes gout) and has been reported to have anti-tumor properties (www.vanderbilt.edu/AnS/psychology/health_psychology/chitosan.htm).

CHAPTER FOUR
MATERIAL AND METHOD

Malachite green is a commercial product of Fluka (Cat No.42000) and it is formula was shown in Figure 4.1.

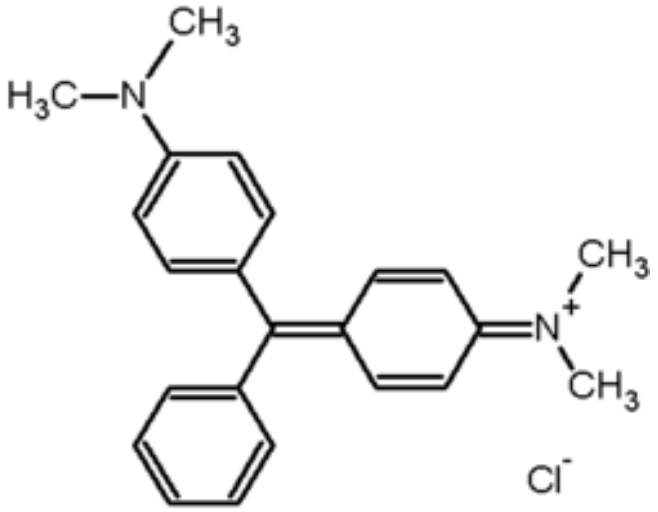


Figure 2.1. Structure chromatic form of malachite green with chlorine salt

Chitosan is a commercial product supplied from Fluka (Cat no: 48165). The chemical structure of chitosan was shown in Figure 4.2.

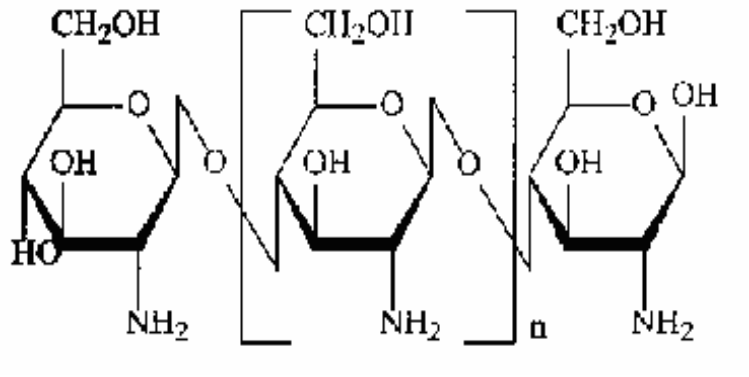


Figure 4.2 Structural formula of chitosan

4.1 Synthesis of Chitosan Bead

Chitosan solution was prepared by dissolving 2.00g chitosan flakes into 50 mL of 5% (V/V) acetic acid solution. It will take about one night to dissolve chitosan completely. Then the solution is dropped into 0.1M NaOH by using pipette tips which and neutralized the acetic acid within the chitosan gel and there by coagulated the chitosan gel get to special uniform chitosan gel beads. The aqueous NaOH solution was stirred using magnetic shaker. The wet chitosan gel beads were extensively rinsed with distilled water to remove any NaOH, filtered and finally air dried to remove the water from the pore structure. The bead were then ground by using grinder and sieved to constant size before use.

4.2 FTIR Study

FTIR spectroscopy was used to obtain the information about the interaction between dried and chitosan sample. Malachite green, chitosan and malachite green loaded chitosan were brought to constant weight in a drying oven at 50°C for 24h. The samples were kept in the desiccators before analysis. 100 mg of fine KBr powder was dried at 110°C and mixed with 1 mg of samples. For pellets, the infrared spectra in the range 4000-400 cm^{-1} were recorded on a Perkin Elmer FTIR spectrophotometer (Spectrum BX-II). The background spectrum of each KBr pellet was obtained by subtracting it from the sample spectra.

4.3 SEM Measurements

Scanning Electron Microscopy (SEM) was carried out in a Jeol JSM 60 SEM attached and X-ray energy dispersive spectrometer, EDS. The surface morphologies of chitosan were studied using a scanning electron microscope at an accelerating voltage of 20 kV. The samples that were used were dried and coated with gold before scanning. For SEM, photographs were taken at different magnifications (between 1000X and 5000X).

4.4 Adsorption from solution Experiments: Determination of Equilibrium Concentration of Malachite Green after Adsorption

Adsorption isotherms determined by using batch equilibrium method. For batch adsorption experiments 0.05 g of chitosan was added 25 mL of malachite green solution. Concentrations of MG in aqueous solution were between 20 and 240μM. The solutions were shaken at 150 rpm in a temperature controlled shaking water bath (Memmert) for 5 h to reach equilibrium under experimental conditions. After 5 h, the samples were taken and centrifuged at 5000 rpm for 15 min. Liquid phases were taken and equilibrium concentration of dye in resultant solution was determined using Shimadzu UV-Visible 1601 model spectrophotometer at λ_{max}=618nm. The amount of MG adsorbed on chitosan was calculated by difference of initial concentration and the equilibrium concentration of MG The same procedures were performed at solution temperatures of 30°C, 40°C and 50°C to find thermodynamic parameters.

In this study, adsorption of malachite green from aqueous solution onto chitosan has been studied. The Langmuir, Freundlich equation were used to fit the equilibrium isotherm. The kinetic and thermodynamic parameters were calculated to find out adsorption rate constant and adsorption mechanism.

CHAPTER FIVE
RESULTS

1M stock solution of MG was prepared by dissolving 0,005g MG in 250 mL solution which was prepared by using 40% ethanol and 60% distilled water to enhance the solubility of the dye. Calibration solutions at appropriate concentrations were prepared by diluting stock solution, and flasks containing the dyes. The absorbance values of calibration solution and calibration curve of MG were shown in Table 5.1 and Figure 5.1, respectively. The absorbencies of calibration solution were measured at 618 nm wavelength using quartz cell. Absorbance values calibration solution were plotted versus concentration.

Table 5.1 Calibration curve of malachite green

Number	C(mg/L)	Absorbance
1	0.927	0.143
2	1.391	0.197
3	1.854	0.279
4	3.708	0.506
5	4.172	0.572
6	4.635	0.637
7	5.099	0.760
8	5.562	0.831
9	6.026	0.900
10	6.489	1.048

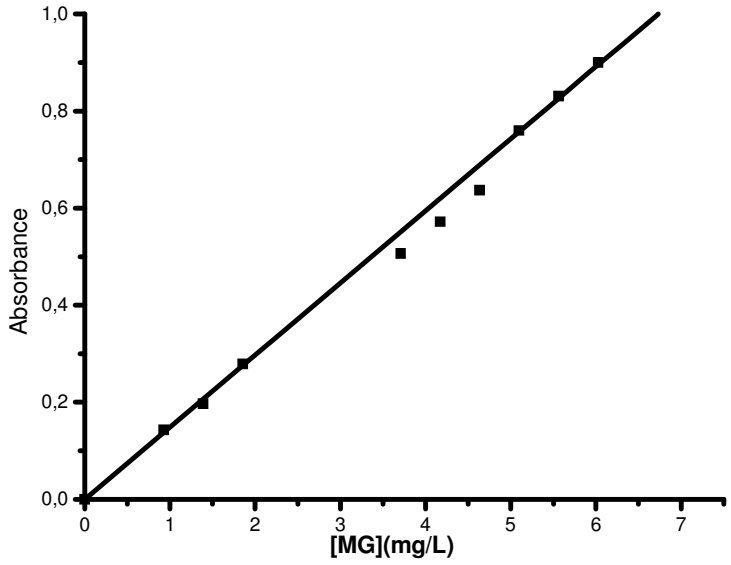


Figure 5.1 Calibration curve of malachite green

5.1 The Effect of Contact Time on Adsorption of Malachite Green onto Chitosan

To determine the optimum contact time for adsorption of malachite green onto chitosan, the equilibrium concentrations were measured at certain times and the amounts of malachite green adsorbed were estimated by the equilibrium concentrations which were obtained. Then, the curve that indicated the effect of contact time on adsorption was plotted the amount of malachite green adsorbed (C_s, mg L^{-1}) measured in the certain (definite) time intervals versus time. Initial work over 8 hours period indicated that equilibrium is almost established within 5h. It can be seen from Figure 5.2, when the contact time was increased; the amount MG adsorbed was also increased.

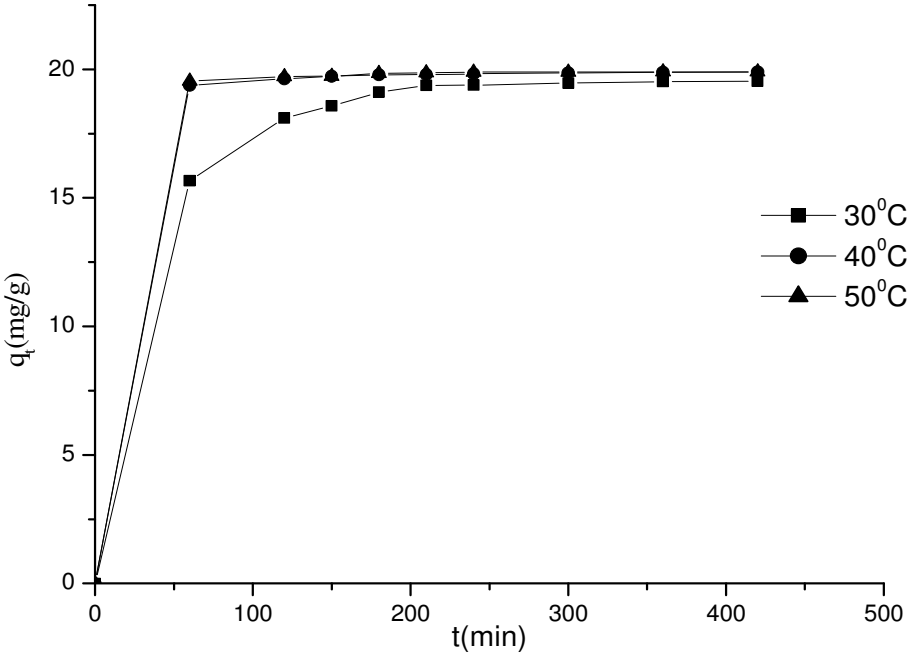


Figure 5.2 Effect of contact time of MG (40 mg L^{-1}) ads. onto chitosan

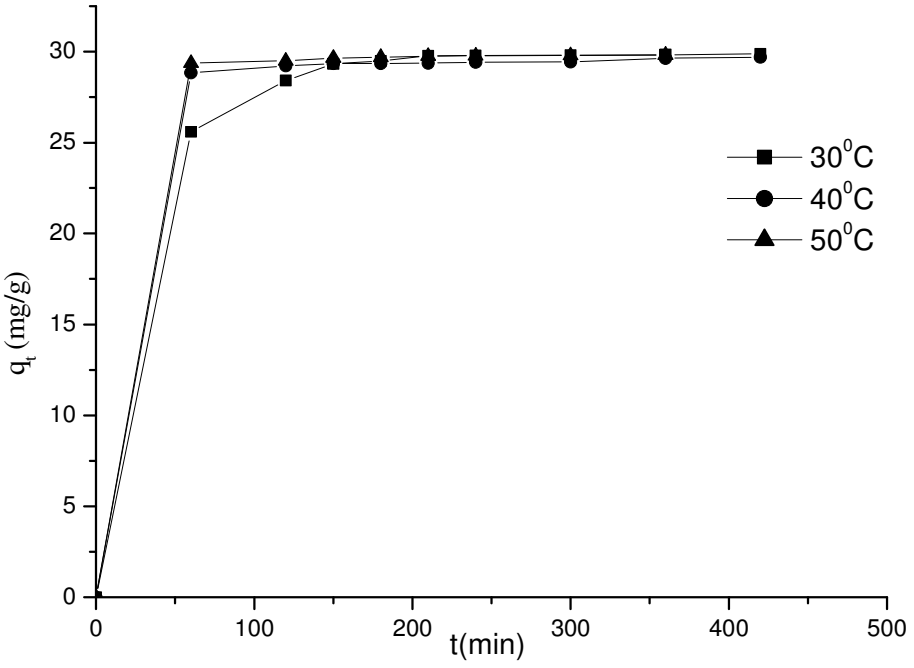


Figure 5.3 Effect on contact time of MG (50 mg L^{-1}) adsorption onto chitosan

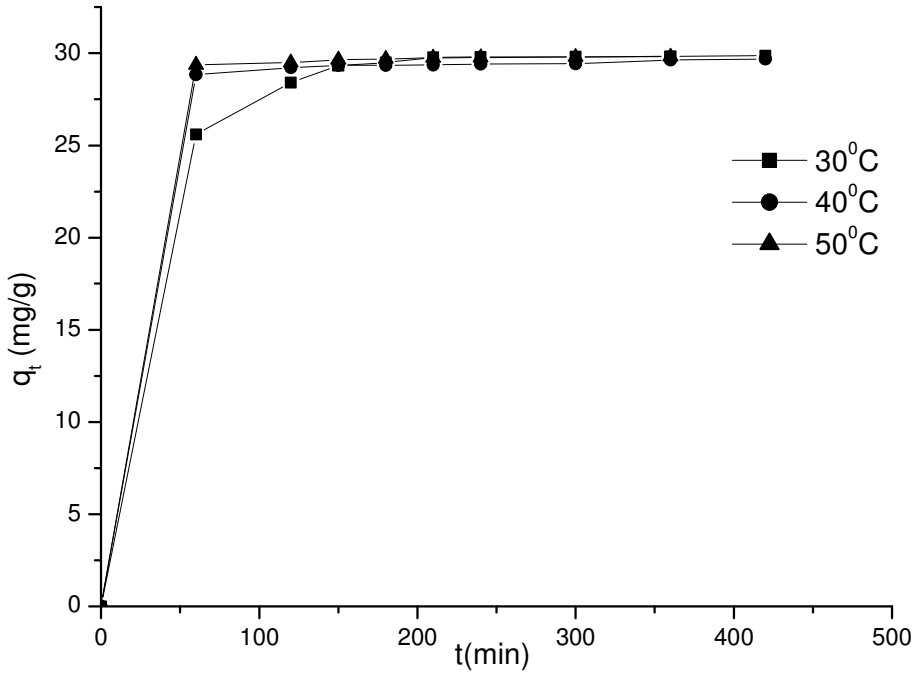


Figure 5.4 Effect of contact time of MG (60 mg L^{-1}) adsorption onto chitosan

5.2 Adsorption of Malachite Green onto Chitosan

Spectrophotometric method was used to determine the concentrations of MG after adsorption. A set of samples for the dye - chitosan suspensions was prepared with different concentrations. The stoppered flasks containing the dye – chitosan suspensions are agitated in a shaker (Memmert) with shaking speed 150 rpm. A portion of the supernatant layer was taken; centrifuged for 10-15 min and equilibrium concentrations of malachite green in the solution after adsorption onto chitosan was determined spectrophotometrically. The data obtained was used to form adsorption isotherms of MG on chitosan.

The adsorption isotherms of MG on chitosan were determined by plotting the amount of MG adsorbed by chitosan (C_s mgL^{-1}) versus equilibrium concentrations of MG (C_e mgL^{-1}). Figure 5.5 shows the MG sorption isotherms at 30, 40, and 50 °C, respectively. In terms of the slope of initial portion of the curves, the shapes of these

isotherms correspond to L type according to the Giles classification (Giles, Mc Ewan & Smith, 1960). The L curve indicates that there is no strong competition from the solvent for sites on the surface. Another possibility is that, if the adsorbate has linear or planar molecules, the major axis is parallel to surface. In that study, it can be easily said that chitosan has a medium affinity for the MG molecules. The curves tend to constant value of C_s and reach a plateau showing the formation of a complete monolayer of MG covering adsorbent surface. The amount of MG adsorbed by chitosan is raised by increasing temperature.

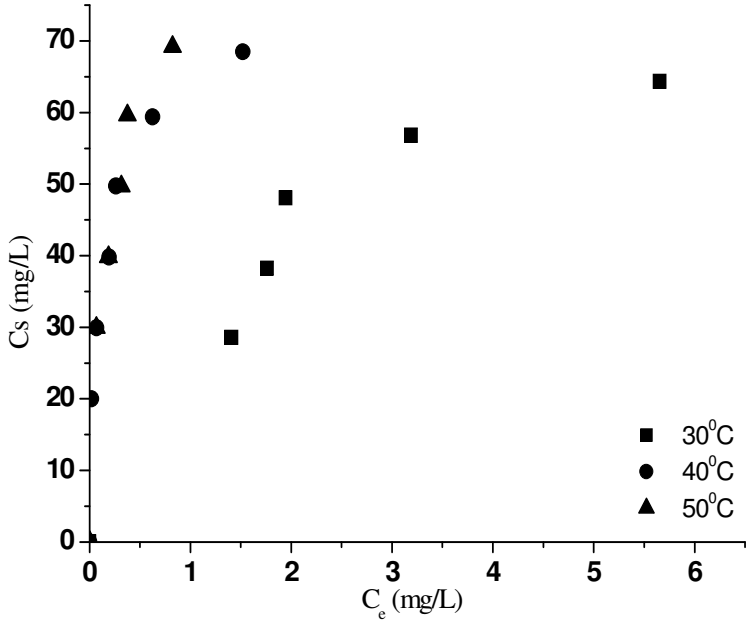


Figure 5.5 Ads. isotherms of MG on chitosan at diff. temperatures

Langmuir and Freundlich equations as written below are applied to evaluate the adsorption data. In order to find sorption capacities of the chitosan, the linear forms these equations are used.

$C_e / C_s = 1 / (C_m L) + C_e / C_m$

$\ln C_s = \ln K_f + n_f \ln C_e$

In these equations;

C_e= the liquid phase concentrations of adsorbate at equilibrium (mg L^{-1}),

C_s= the solid phase concentrations of adsorbate at equilibrium (mg L^{-1}),
C_m= the maximum adsorption capacity (maximum amount that can be adsorbed by adsorbent as a monolayer (mg L^{-1}),
L= Langmuir constant regarding the adsorption energy,
K_f = adsorption capacity,
n_f =heterogeneity factor (adsorption intensity) (a measurement of linearity).

C_m and L parameters are obtained by plotting C_e/C_s versus C_e for the adsorption process of M.G onto chitosan at different temperatures (see Fig. 5.6). The sorption parameters of M.G onto chitosan at corresponding to Langmuir equation were summarized in Table 5.2. C_m (maximum adsorption capacity) values are 93.545 mg L^{-1} at 30°C; 74.833 mg L^{-1} at 40°C; 82.169 mg L^{-1} at 50°C respectively. In addition, L values are 0.409 mg L^{-1} at 30°C; 8.745 mg L^{-1} at 40°C and 6.085 mg L^{-1} at 50°C respectively.

It can be added that although the adsorption of MG onto chitosan can be fitted by Langmuir, the assumptions of these isotherms may not be purely satisfied (Seki, 2002).

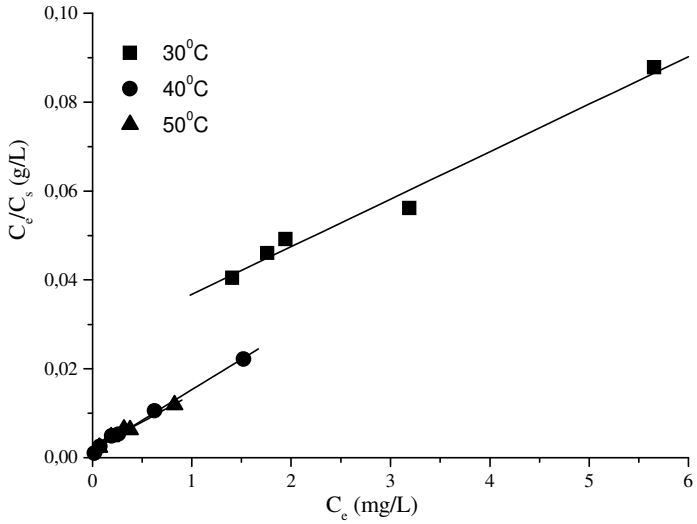


Figure 5.6 Langmuir isotherms for adsorptions of MG onto chitosan at different temperatures

Table 5.2 The sorption parameters of Langmuir equation for MG onto chitosan at different temperatures

Temperature(°C)	**R^2**	**C_m (mg L^{-1})**	**L (g L^{-1})**
30	0.982	93.55	0.41
40	0.996	72.83	8.75
50	0.982	82.17	6.09

To determine the adsorption process is favorable or unfavorable, for the Langmuir type adsorption process, the isotherm shape can be classified by a term 'R_L' a dimensionless constant separation factor, which is defined as below;

$R_L = 1/1(1+a_L C_0)$

where,

a_L=Langmuir isotherm constant ,

C_0 = Initial malachite green concentration (mg L^{-1}).

The shapes of the isotherms for $0 < R_L < 1$, $R_L > 1$, $R_L = 1$ and $R_L = 0$ are favorable, linear and irreversible respectively (Weber & Chakkravorti, 1974).

The values of R_L (dimensionless separation factor) at different temperatures are reported in Table 5.3. The values of R_L were between 0 and 1. These values indicated that favorable adsorption for MG occurred

Table 5.3 Dimensionless separation factors for adsorption of MG onto chitosan at different temperatures

Temperature(°C)	**a_L/L (mg^{-1})**	**C_0 (mmol L^{-1})**	**R_L**
30	0.41	40	0.058
40	8.75	40	0.003
50	6.09	40	0.004

In order to determine the constants K_f (relative sorption capacity) and n_f (measure of the linearity of the sorption) the linear form of Freundlich equation can be given as

$\ln C_s = \ln K_f + n_f \ln C_e$

A graph indicating adsorption of MG onto chitosan which is formed by plotting $\ln C_s$ versus $\ln C_e$ is shown in the Figure 5.7. The correlation coefficients R^2 are greater than 0.817. Based on R^2 values, the fit of Freundlich is not good as Langmuir equation.

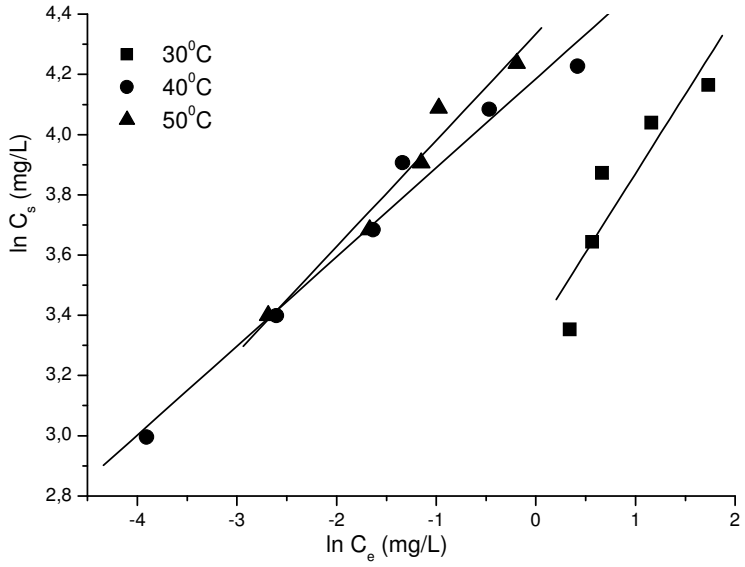


Figure 5.7 Freundlich isotherms for adsorption of MG onto chitosan at different temperatures

Table 5.4 The sorption parameters of Freundlich equation for adsorption of MG onto chitosan at different temperatures

Temperature(°C)	**R^2**	**K_f (mgL^{-1})**	**n_f**
30	0.817	28.38	0.53
40	0.977	65.76	0.30
50	0.966	76.23	0.35

Freundlich constants were shown in Table 5.4. As can be seen from Table 5.4, K_f values are raised by increasing temperature. This result indicates that adsorption capacities of Chitosan decrease when temperatures decrease. It can be easily understood that MG is more adsorbed at 50°C than that of 40°C and 30°C. It can be

said that the values of n_f are smaller than 1, reflecting favorable adsorption. (Ghiaci, Abbaspur, Kra & Seyedeyn, 2004).

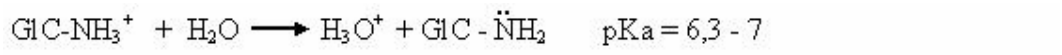
Both these theories suffer from the disadvantage that equilibrium data over a wide concentration range can not be fitted with single set of constant (Mc Kay et. al, 1896). The n_f values are less than 1 in the form of linear Freundlich equation. The n_f is indicator of heterogeneity factor. If the value of n_f is equal unity, the adsorption is linear. It indicates that adsorption sites are not homogeneous in energy.

The correlation factors (R^2) indicated that better applicability was obtained using linearized Langmuir and Freundlich isotherms, respectively.

5.3 Effect of pH on Adsorption of MG onto Chitosan

The influence of pH on the malachite green adsorption onto chitosan was studied while the malachite green concentration, shaking time and amount of chitosan were fixed at 50 mg L^{-1}, six hours and 0.05 g respectively. The variation of dye adsorption onto chitosan over a pH range of 2.10 – 10.99 is shown in Figure 5.8. The result reveals that the adsorption of malachite green increases from %18.80 to %99.38 with an increase in pH of the solution from 2.10 to 10.99 and the remains almost constant. The adsorption of the charged dye groups onto the chitosan is primarily influenced by the pH value at the solution.

The Chitosan had positive charge in acidic condition.



Since the pKa value at chitosan (GlC–NH_3^+) is in the pH range of 6.3–7, the amino groups of chitosan are protonated at low pH values. Malachite green is a cationic basic dye as denoted by the presence of the positive nitrogen ion enters the aqueous solution ensuring that the dye has an overall positive charge. In acidic pH, cationic chitosan repulse the cationic dye, for that reason the adsorption of malachite green onto chitosan is low in acidic pH. However the pH is increased to basic pH

values, the amino groups of chitosan are deprotonated. In this case, the interaction between cationic MG and the pair of electrons of nitrogen present in the structure of chitosan occurs. It is clear that the adsorption of dye onto chitosan at basic pH values is high.

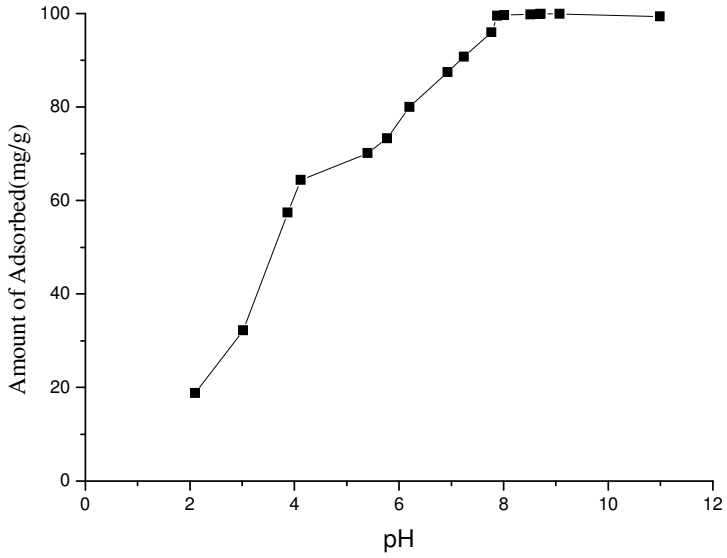


Figure 5.8 pH effects on adsorption of MG onto chitosan (30º, 50 mg L^{-1} MG)

5.4 Adsorption Kinetics

In order to optimize the design of an adsorption system of MG onto chitosan, it is important to establish the most appropriate correlations for the equilibrium data for each system. In this respect, several kinetic models including the pseudo first order equation, pseudo second order equation, and intraparticle diffusion model were applied to find out adsorption mechanism.

$1/q_t = (k_1/q_1)(1/t) + 1/q_1$ Pseudo first order

$t/q_t = 1/k_2.q_2^2 + (1/q_2).t$ Pseudo second order

$q_t = k_p t^{0.5} + C$ Intraparticle Diffusion

where,

q_t is the amount of MG adsorbed (mg g^{-1}) onto chitosan at various time t ,

q_1 is the maximum adsorption capacity (mg g^{-1}) for the pseudo first order adsorption,

k_1 is the pseudo first order rate constant for the adsorption process (min^{-1}),

q_2 is the maximum adsorption capacity (mg g^{-1}) for the pseudo second order adsorption,

k_2 is the rate constant of pseudo-second-order for the adsorption (g mg^{-1} min^{-1}),

k_p is the intraparticle diffusion rate constant (mg g^{-1} $min^{-0.5}$),

C is the intercept for the intraparticle diffusion model (mg g^{-1}).

The straight-line plots of $1/q_t$ versus 1/t for the pseudo –first order reaction and t/q_t versus t for the second order reaction for the adsorption MG onto chitosan have also been tested to obtain the rate parameters. The k_1, k_2, q_1, q_2 and correlation coefficients R_1^2 and R_2^2 of MG under different conditions were calculated from these plots and are given in Tables 5.5, 5.6, 5.7, 5.8, 5.9, 5.10 and 5.11, respectively (Özcan &Özcan, 2004).

Table 5.5 The pseudo first order parameters for MG (40mg L^{-1}) at different temperatures

Temperature(°C)	$\mathbf{R^2}$	$\mathbf{k_1}$ **(min** $^{-1}$**)**	$\mathbf{q_1}$ **(mg** $\mathbf{g^{-1}}$**)**
30	0.972	18.89	20.75
40	0.987	1.99	20.00
50	0.942	1.45	19.99

Table5.6 The pseudo first order parameters for MG (50mg L^{-1}) at different temperatures

Temperature(°C)	$\mathbf{R^2}$	$\mathbf{k_1}$ **(min** $^{-1}$**)**	$\mathbf{q_1}$ **(mg** $\mathbf{g^{-1}}$**)**
30	0.958	30.61	16.41
40	0.941	2.54	25.04
50	0.810	0.98	24.86

Table 5.7 The pseudo first order parameters for MG (60mg L^{-1}) at different temperatures

Temperature(°C)	**R^2**	**k_1 (min^{-1})**	**q_1 ($mg\ g^{-1}$)**
30	0.953	12.61	32.25
40	0.906	25.59	37.034
50	0.861	1.08	29.85

Table 5.8 The pseudo second- order parameters for MG (40mg L^{-1}) at different temperatures

Temperature(°C)	**R^2**	**k_2 ($gmg^{-1}\ min^{-1}$)**	**q_2 ($mg\ g^{-1}$)**
30	0.989	0.01	19.53
40	0.999	0.05	19.49
50	1.000	0.05	19.95

Table 5.9 The pseudo second order parameters for MG (50mg L^{-1}) at different temperatures

Temperature(°C)	**R^2**	**k_2 ($g\ mg^{-1}\ min^{-1}$)**	**q_2 ($mg\ g^{-1}$)**
30	0.998	0.01	15.22
40	0.999	0.03	24.94
50	1.000	0.04	24.98

Table 5.10 The pseudo second order parameters for MG (60mg L^{-1}) at different temperatures

Temperature/°C	**R^2**	**k_2 /g $mg^{-1}\ min^{-1}$**	**q_2 ($mg\ g^{-1}$)**
30	0,998	0.01	30.21
40	0.999	0.02	29.85
50	1.000	0.04	29.85

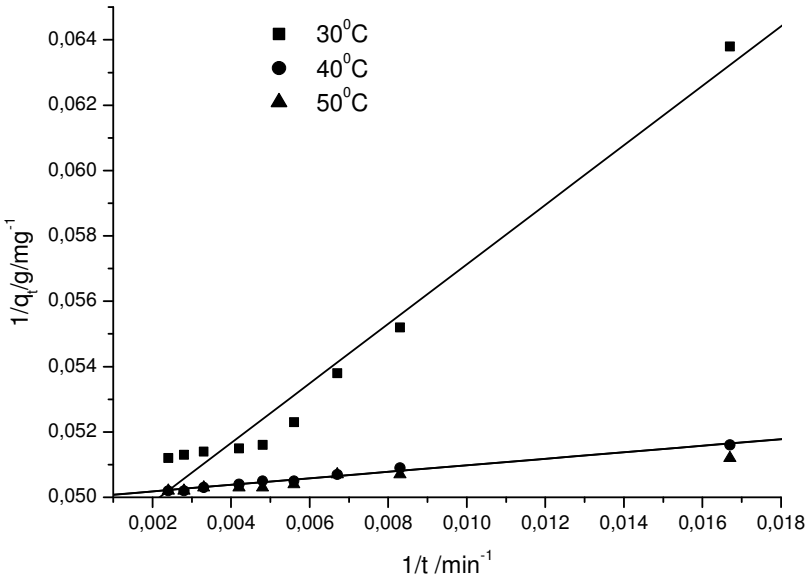


Figure 5.9 Pseudo-first-order plot for ads. of MG (40mg L^{-1}) onto chitosan at different temperatures

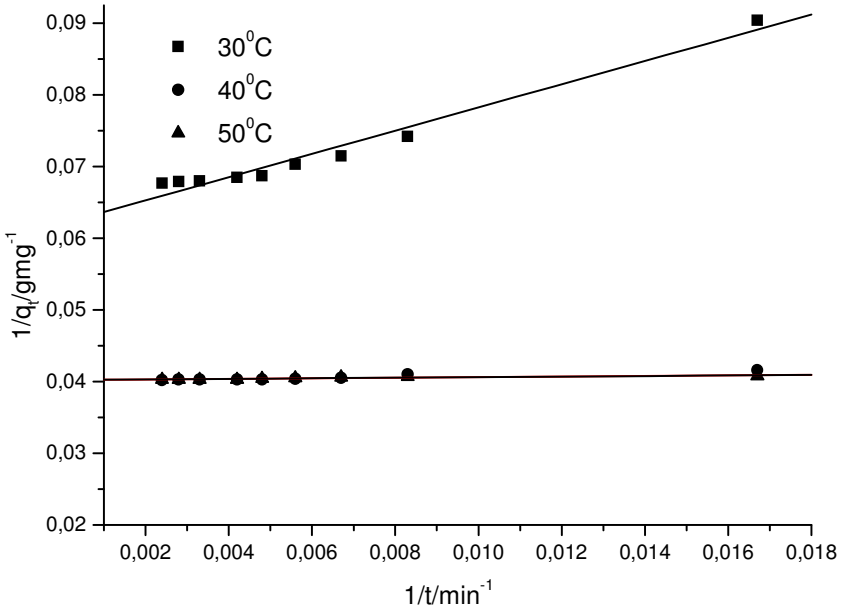


Figure 5.10 Pseudo first order plot for ads. of MG (50mg L^{-1}) onto chitosan at different temperatures

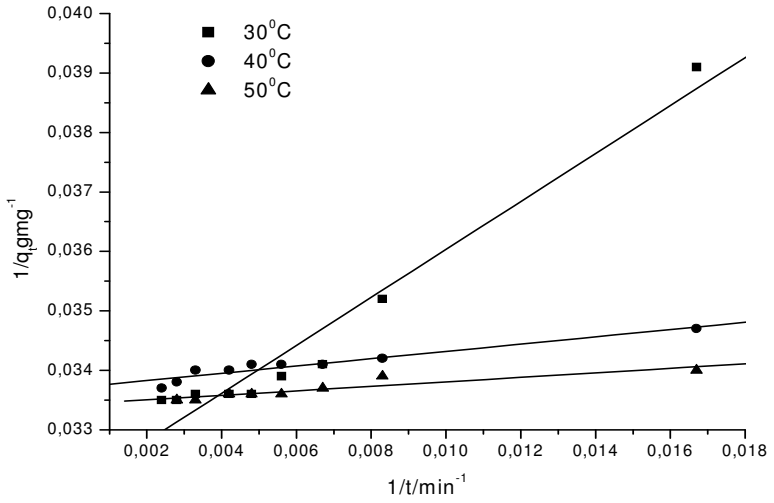


Figure 5.11 Pseudo first order plot for ads. of MG (60mg L^{-1}) onto chitosan at different temperatures

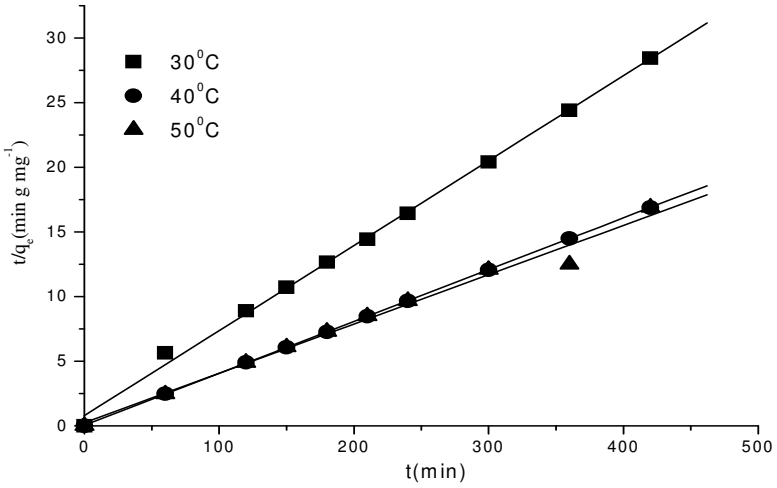


Figure 5.12 Pseudo second order plot for ads. of MG(40mg L^{-1}) onto chitosan at different temperatures

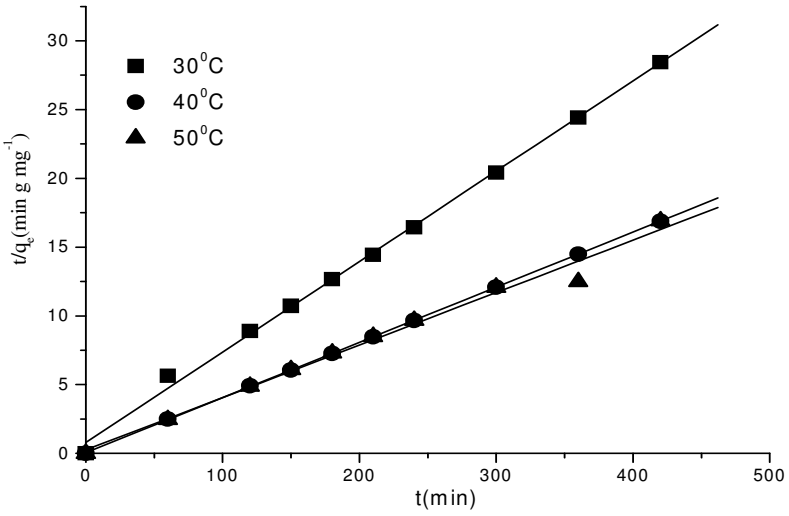


Figure 5.13 Pseudo second order plot for ads. of MG (50mg L^{-1}) onto chitosan at different temperatures

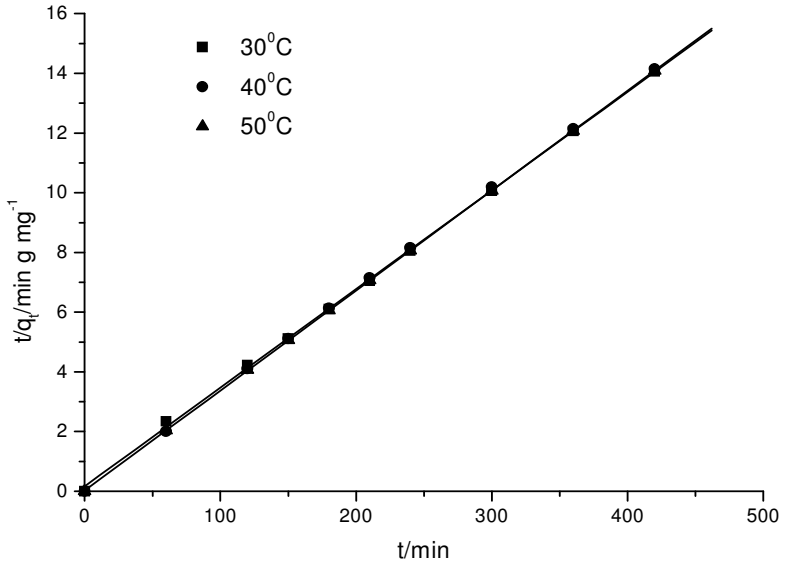


Figure 5.14 Pseudo second order plot for ads. of MG (60 mg L^{-1}) onto chitosan at different temperatures

As can be seen Table 5.5, 5.6, 5.7, 5.8, 5.9 and 5.10, respectively, the coefficients (R_1^2) for pseudo first order kinetic model are between 0.810 and 0.987 and the correlation coefficients (R_2^2) for pseudo-second kinetic model are between 0.989 and

1.000. These results show that the adsorption system obeys the pseudo second order kinetic model.

Adsorption kinetics are usually controlled by different mechanisms, of which the most limiting are the diffusion mechanisms, including the initial curved portion, attributed to rapid external diffusion or boundary layer diffusion and surface adsorption, and the linear portion, q gradual adsorption stage due to intraparticle diffusion starts to decrease due to the low concentration in solution as well as fever available adsorption sites.

The rate-limiting step may be due to intraparticle diffusion. The rate constant for the intraparticle diffusion was obtained using the proper equation.

C gives an idea about the boundary layer thickness. If the intraparticle diffusion is involved in the adsorption process, then a plot the square root of time ($t^{1/2}$) versus the uptake (q_t) would result in a linear relationship and the particle diffusion would be the controlling step if this line passed through the origin.

When the plots do not pass through the origin, this is indicative of some degree of boundary layer control and the further show that the intraparticle diffusion is not the only rate-controlling step, but also other processes may control the rate of adsorption, all of which may be operating simultaneously.

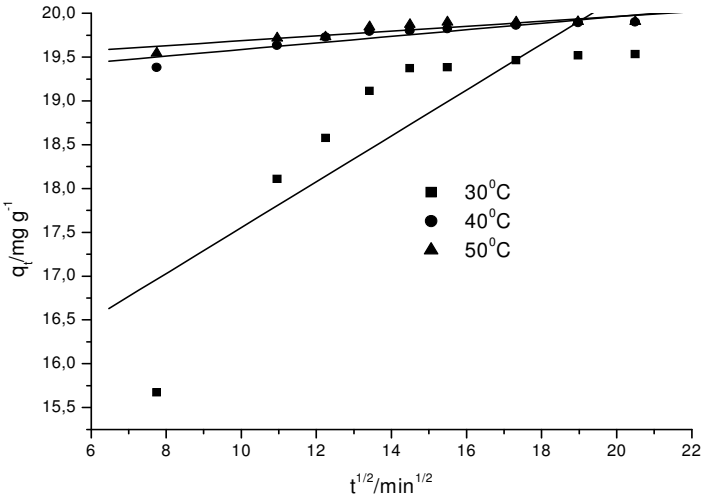


Figure 5.15 Intraparticle diffusion plot for MG (40mgL^{-1}) onto chitosan at different temperatures

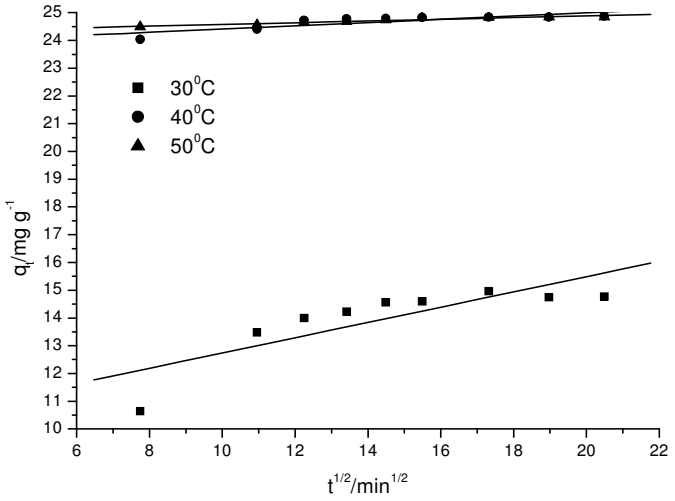


Figure 5.16 Intraparticle diffusion plot for MG (50mgL^{-1}) onto chitosan at different temperatures

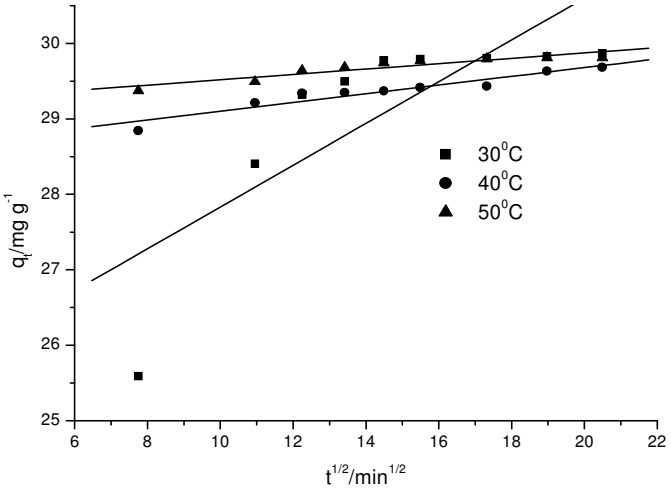


Figure 5.17 Intraparticle diffusion plot for MG (60mgL^{-1}) onto chitosan at different temperatures

The slope of the linear portion from Figures 5.15, 5.16 and 5.17 can be used to derive values for the rate parameters, k_p, fort he intraparticle diffusion, given in Tables 5.11, 5.12 and 5.13, respectively.

Table 5.11 Intraparticle diffusion parameters for MG (40mg L^{-1}) onto chitosan at diff. temperatures

Temperature(°C)	$\mathbf{R}^2$	$\mathbf{k}_p$ **(mg g^{-1} min$^{-1/2}$)**	**C (mg g^{-1})**
30	0.840	0.26	14.94
40	0.916	0.04	19.21
50	0.898	0.03	19.41

Table 5.12 Intraparticle diffusion parameters for MG (50mg L^{-1}) onto chitosan at diff. temperatures

Temperature(°C)	$\mathbf{R}^2$	$\mathbf{k}_p$ **(mg g^{-1} min$^{-1/2}$)**	**C (mg g^{-1})**
30	0.821	0.27	10.04
40	0.954	0.03	24.27
50	0.844	0.06	23.83

Table 5.13 Intraparticle diffusion parameters for MG (60mg L^{-1}) onto chitosan at dif. temperatures

Temperature(°C)	**R^2**	**k_p (mg g^{-1} $min^{-1/2}$)**	**C (mg g^{-1})**
30	0.797	0.277	25.07
40	0.954	0.058	28.52
50	0.627	0.036	29.16

From Tables 5.11, 5.12 and 5.13, it is understood that the intraparticle diffusion is not the rate controlling step. Other process may control the rate of adsorption (Mahramanlioğlu, et. al, 2003). The correlation coefficients (R_p^2) for the intraparticle diffusion model are between 0.627 and 0.954. The linear portions of curves do not pass through the origin. This indicates that the intraparticle diffusion is not the only rate controlling step and adsorption mechanism of M.G onto chitosan complex. The larger the intercept (C value), the greater is the boundary layer effect. C values are for example; 25.07, 28.523 29.16 mg g^{-1} at 30, 40 and 50°C for 60mg L^{-1} respectively. As can be seen from tables the values of the sorption capacity at equilibrium q_1 and q_2 are nearly same. For initial concentration of Malachite green, q_2 values are increased when the temperature is increased. This result is not observed for the other initial concentrations. Also, as can be seen from Freundlich equation, results and the adsorption isotherms for malachite green onto chitosan indicate that the adsorption capacity is increased by increasing the temperature of the malachite green solutions.

5.5 Thermodynamic Parameters of Adsorption

The thermodynamic parameters of the adsorption process are obtained from experiments at various temperatures. It is essential to clarify the change of thermodynamic parameters. Gibbs energy change, ΔG° are estimated by applying thermodynamic equation (Özcan, et. al., 2004).

$$\Delta G^0 = -RT\ln K_d$$

where ,

K_d = equilibrium constant at temperature T,

R= Gas constant (8.314 J $mol^{-1} K^{-1}$),

T=Absolute temperature (K).

For each temperature, the same t values were selected (360 min) and from this value, firstly q_t and then C_s and C_e values were calculated by using pseudo second order equation. K_d was estimated using the following equation;

$K_d = C_s/C_e$

where,

C_e=Equilibrium concentration,

C_s= The amount of adsorbed.

Table 5.14 The equilibrium constant (K_d) for adsorption of MG onto chitosan at different temps. in 6 hours

Temperature(°C)	**$C_s x10^4$ ($molL^{-1}$)**	**$C_e x10^4$ ($molL^{-1}$)**	**K_d**	**lnK_d**	**1/T(K^{-1})**
30	29.437	20.563	1.43	0.36	0.0033
40	49.688	0.312	159.46	5.07	0.0032
50	49.830	0.170	293.29	5.68	0.0031

To determine the values of ΔH^0 and ΔS^0, the van't Hoff equation is used;

$\ln K_d = (\Delta S^0/R^0) - (\Delta H^0/RT)$

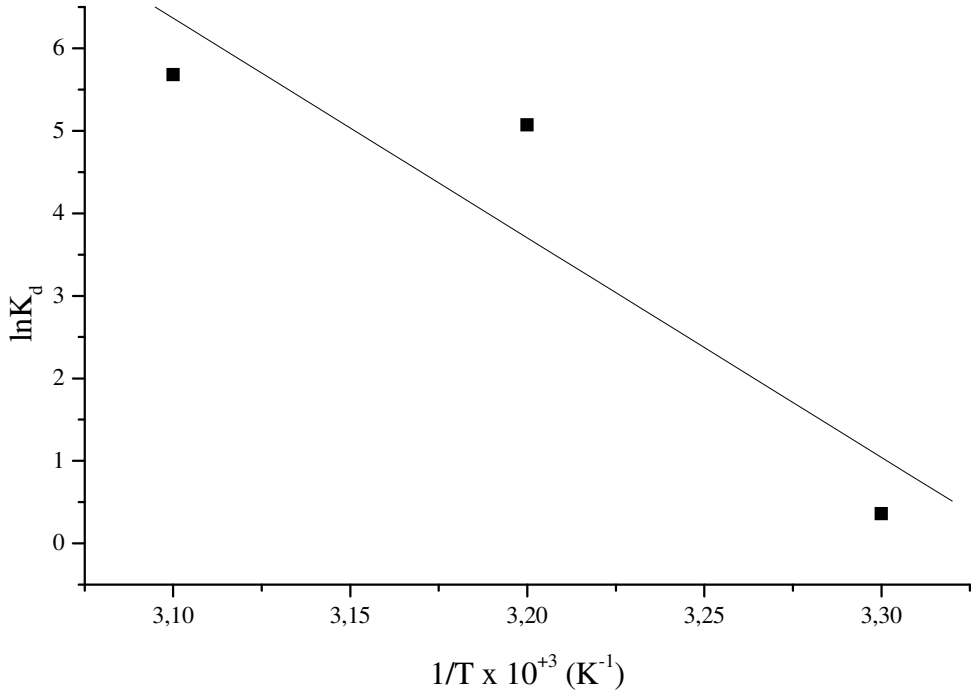


Figure 5. 18. van't Hoff plot of ln K_d vs 1/T for adsorption of malachite green (C_0= 50mg L^{-1}) onto chitosan

Thermodynamic parameters calculated with the second-order rate constant are presented Table 5.15.

Table 5.15 Thermodynamic parameters for adsorption of MG onto chitosan

Temperature(°C)	**ΔH^0 (kJ mol^{-1})**	**ΔS^0 (mol^{-1} K^{-1})**	**ΔG^0 (J mol^{-1})**
30	221	739	-904
40			-13198
50			-15256

The Gibbs free energy demonstrates a spontaneous and favorable adsorption process. The higher negative value reflects a more energetically favorable adsorption (Aksu, et al., 2004). The Gibbs free energy value at 50°C is the highest negative

value than the values of other temperatures. For that reason, more energetically favorable adsorption is occurred 50°C.

As shown Table 5.15, the values ΔH^0 and ΔS^0 were positive for adsorption of MG onto chitosan. The positive value of ΔH^0 indicates that the adsorption process is endothermic in nature and the positive value ΔS^0 showed the increase in degree of freedom or increases the disorder of adsorption process. The positive value of ΔS^0 suggests increase randomness at solid/solution interface and significant changes occur in the internal structure of the adsorbent through the adsorption of M.G onto chitosan (Özcan, et.al., 2004).

The activation energy, E_a, was obtained from an Arrhenius plot. Arrhenius equation is shown as below;

$k_2 = Ae^{-Ea/RT}$ or

$\ln k_2 = \ln A - E_a/RT$

where , k_2 == Rate constant of pseudo second order adsorption (g mg^{-1} min^{-1}),

A=The Arrhenius factor,

R= Gas constant (8.314 J mol^{-1} K^{-1}),

T= Absolute temperature (K).

The plot of $\ln k_2$ versus 1/T for the adsorption of MG onto chitosan was applied to obtain the activation energy, E_a from the slope.

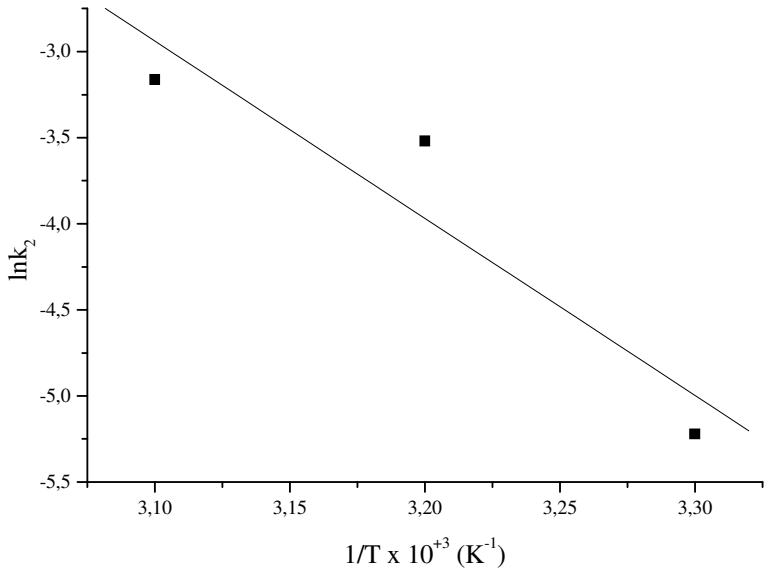


Figure 5.19 The Arrhenius plot for MG adsorption onto chitosan

Adsorption energy for MG adsorption onto chitosan is 85.57 kJ mol^{-1} (the correlation coefficient is 0.936). This activation energy value is not between 5-40 kJ mol^{-1} values. Since it is high, it is understood that the chemical adsorption mechanism is occurred. It can be easily said that the positive value of E_a represents the nature of chemical adsorption of MG onto chitosan; there is an energy barrier in the adsorption process.

5.6 SEM Analysis

Surface morphology of the adsorbent, chitosan was investigated by using JEOL SEM Analysis Instrument in the Metallurgy and Materials Engineering Faculty of Dokuz Eylül University, İzmir, Turkey. The samples were coated with gold before the analysis. Acceleration voltage was applied as 15 kV.

Surface Morphology of synthesized chitosan beads can be seen in Figures 5.20, 5.21, 5.22, 5.23 and 5.24 at different magnifications**.**

5.6.1 Surface Morphology

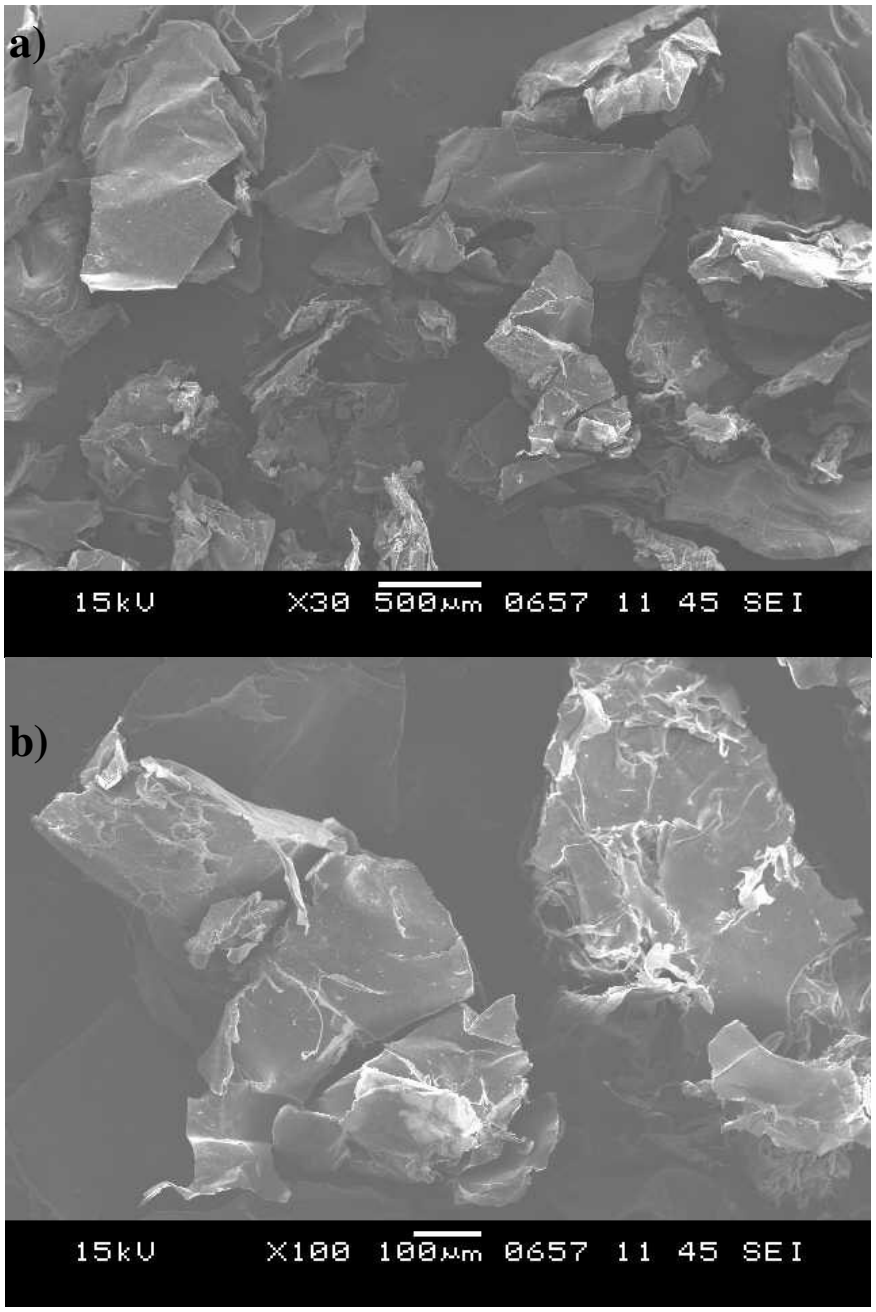


Figure 5.20 SEM images showing the surface morphologies of the chitosan beads (at 30X and 300 X magnifications)

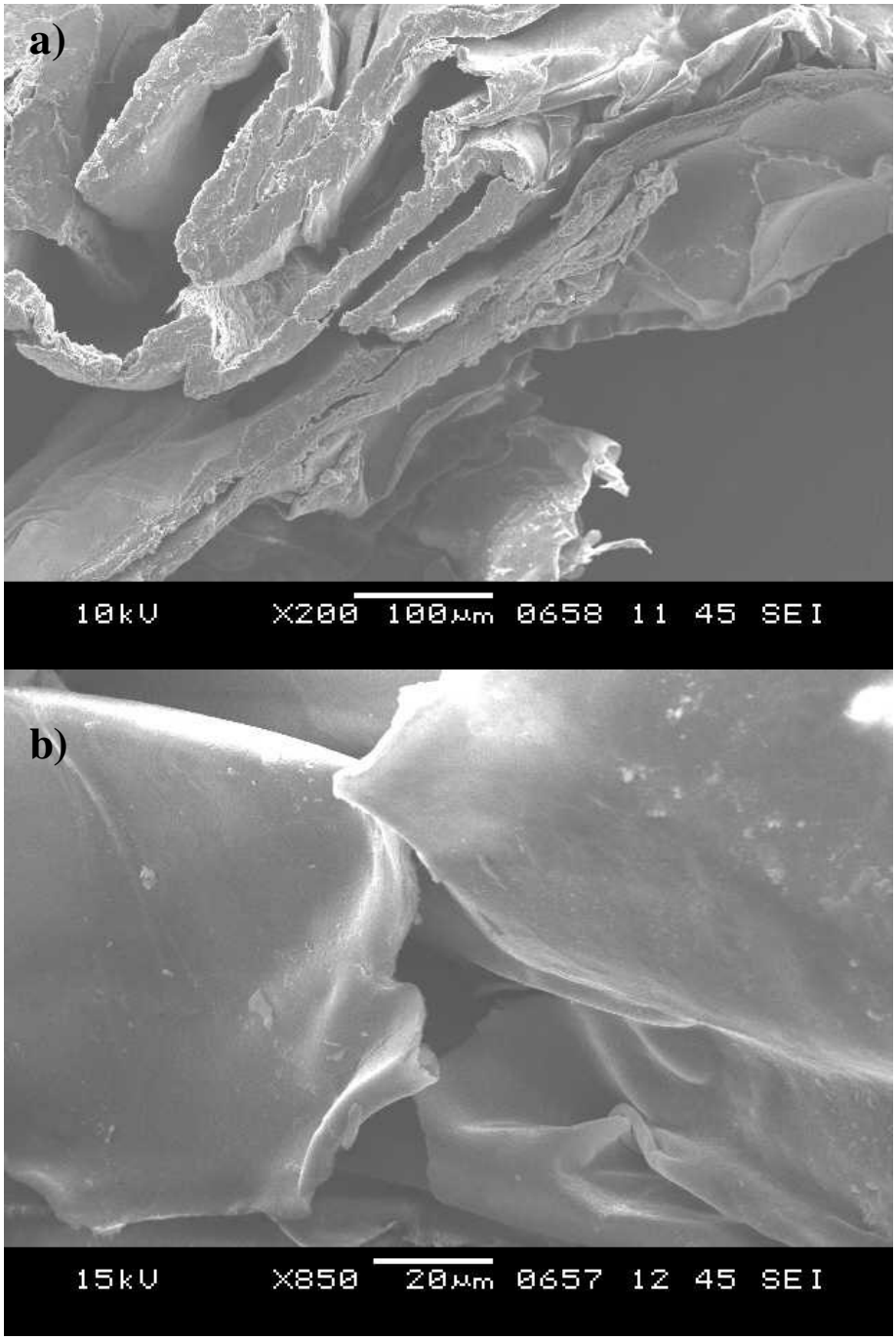


Figure 5.21 SEM images showing the surface morphologies of the chitosan beads (at 850 and 200X magnifications)

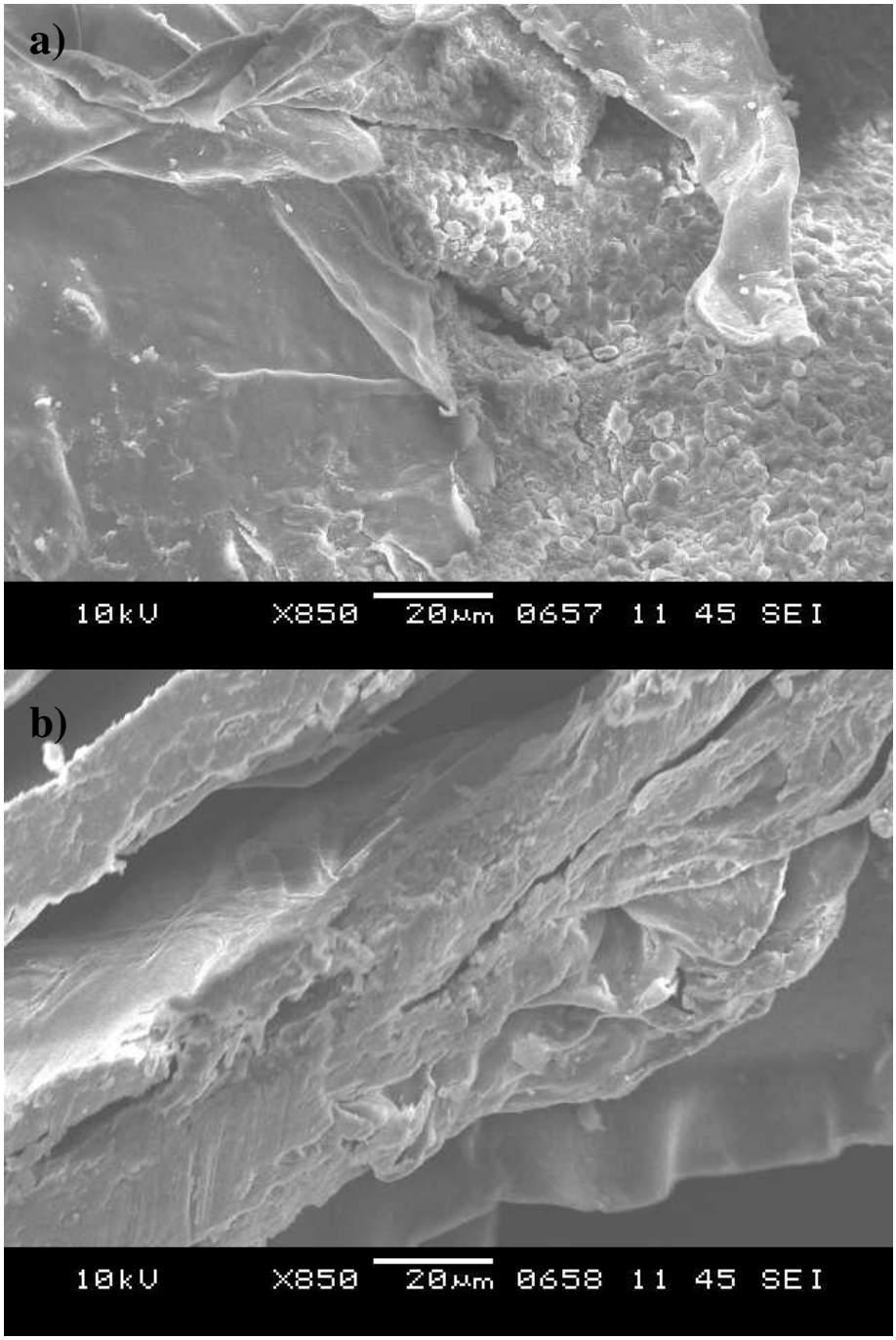


Figure 5.22 SEM images showing the surface morphologies of the chitosan beads (at 850 X magnifications)

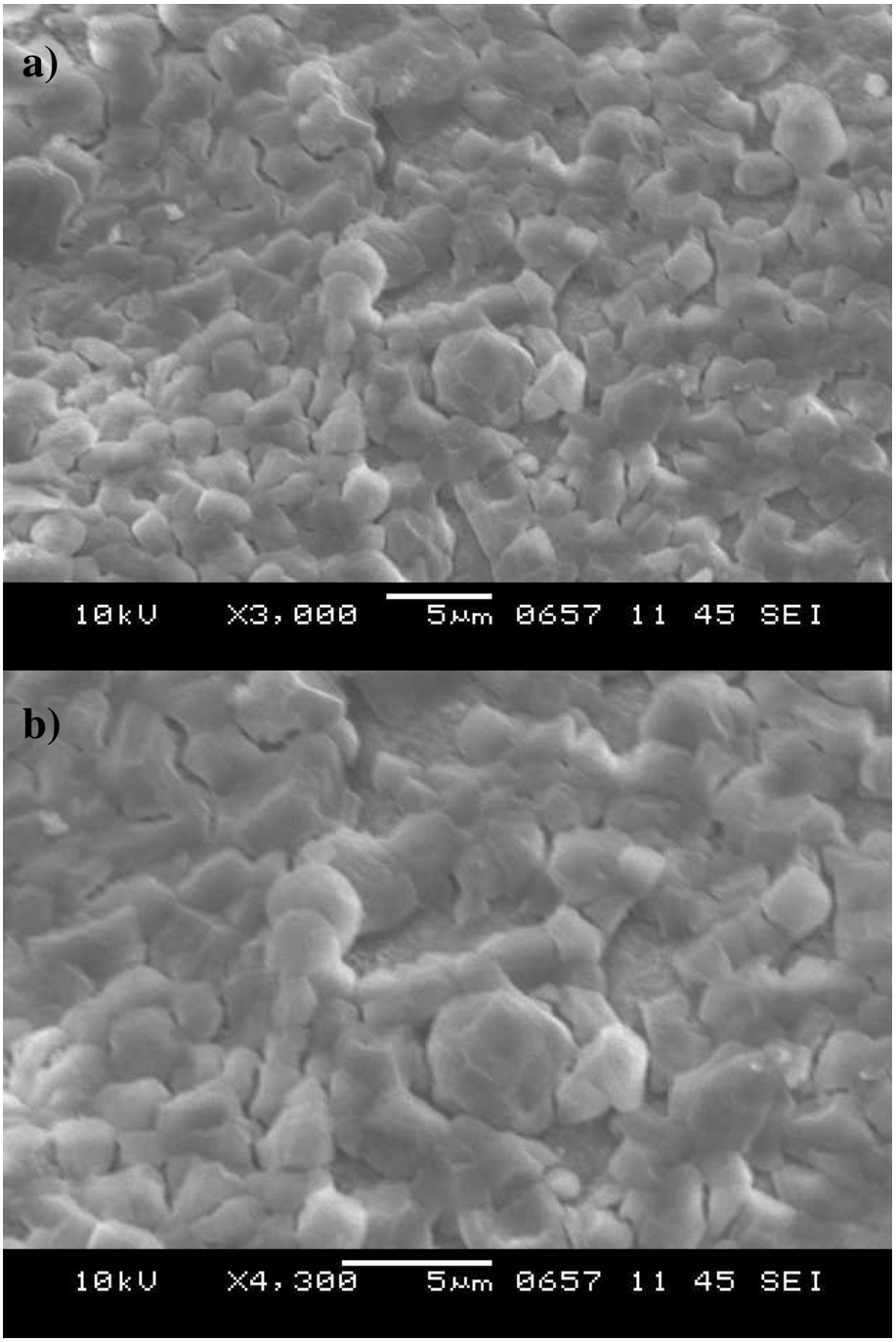


Figure 5.23 SEM images showing the surface morphologies of the chitosan beads (at 3000X and 4300 X magnifications)

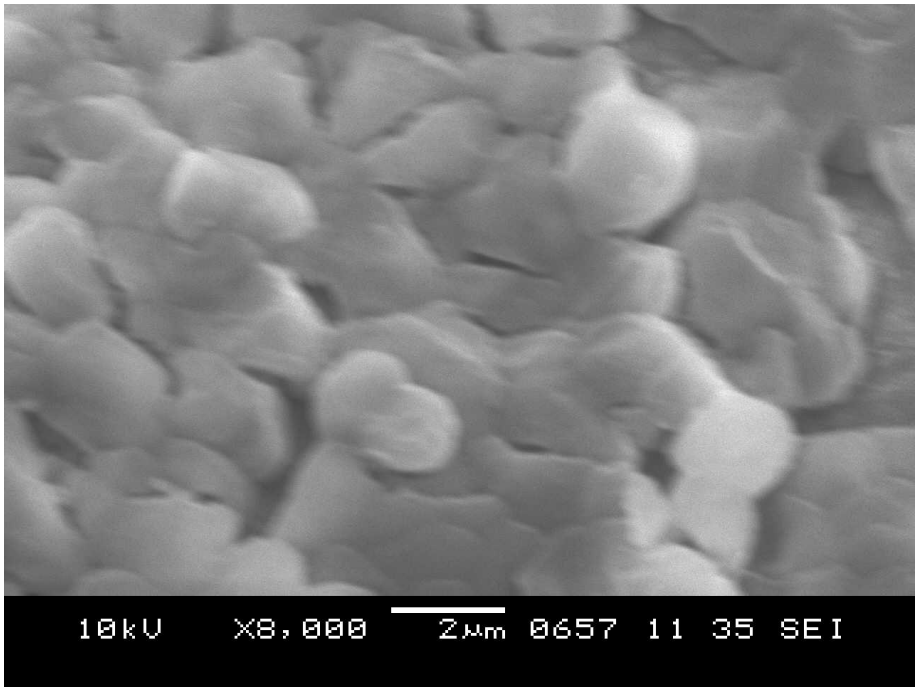


Figure 5.24 SEM images showing the surface morphologies of the chitosan beads (at 8000 X magnifications)

As can be seen from Figures 5.20a and 5.20b (at 30X and 100X) magnifications macroscopically synthesized chitosan beads are generally spherical. The chitosan particles have different size and dimensions. Some of the particles are greater than 500 µm. As shown in Figures 5.21a and 5.22b (at 200X and 850X magnifications respectively), large pores exist on the surface of chitosan bead. In Figure 5.21b (at 850X magnification), micro-pores at about 20 µm can be seen easily. Those pores are very suitable places for the sorption of MG. In these figures, the shapes of chitosan are not spherical. Small flakes were bended in some places and large pores occurred.

As can be seen from Figures 5.23a, 5.23b and 5.24 (at 3000X, 4300X and 8000X magnifications respectively), pores with different size were observed. In addition to these, as can be seen from Figures 5.23 and 5.24, micro-particles were observed. Some of them are spherical and adhere to each other and held together. As shown in Figure 5.24, pores smaller than 1 µm are observed on the surface of the chitosan bead.

5.7 FTIR Analysis

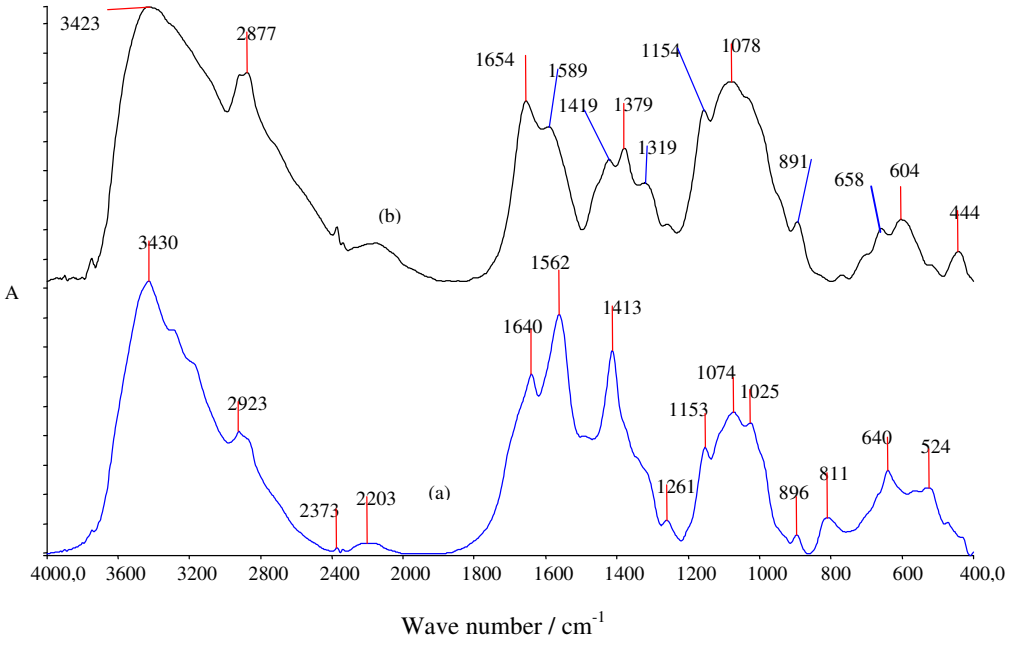


Fig 5.25 FTIR spectra of chitosan bead (a) before and (b) after adsorption of MG

The FTIR spectra of chitosan bead before and after adsorption were shown in Figure 5.25. The wide band at 3430 cm^{-1} shown in the spectrum of chitosan bead is attributed to stretching vibration of hydroxyl group of chitosan. This band was decreased to 3423 cm^{-1} when MG was adsorbed. It may indicate a hydrogen bond between malachite green and OH groups of chitosan. The small band at 3748 cm^{-1} is due to stretching vibration of N-H groups. It is not seen exactly in the spectrum of Chit-MG. The band at 2923 cm^{-1} shown in Figure 5.25 is assigned to the C-H stretching vibration of polymer backbone. There was significant decrease for that band in the spectrum of malachite green (2877 cm^{-1}). This can be considered as the evident for the interaction between chitosan and MG cation. The band at 1413 cm^{-1} in the spectrum of chitosan bead is due to C-H bending which was appeared as duplicated at 1419 cm^{-1} and 1379 cm^{-1} in the spectrum of chitosan bead after adsorption. The band at 1379 cm^{-1} in the spectrum of Chit-MG is assigned to a symmetrical deformation of the CH_3 group. The bands observed at 1640 cm^{-1} and 1562 cm^{-1} correspond to N-H bending vibrations. These bands increased to 1654

cm^{-1} and 1589 cm^{-1} when the adsorption of MG occurs. These changes may be owing to weak interactions between MG and chitosan. Presumably it can be claimed that hydrogen bonding occurs between nitrogen and hydrogen of chitosan and MG. As was indicated by Paulino et al. 2006, the band at 1562 cm^{-1} has a larger intensity than at 1640 cm^{-1}, which suggests effective deacetylation. Note in the spectrum of chitosan that presence of two bands, one at 1153 cm^{-1} and another at 1074 cm^{-1}, probably indicates stretching vibrations of C-O group. The first band did not demonstrate any changes. Besides in the second band, a small change was observed. It can be said that no interaction occurs between C-O groups of chitosan and MG cation.

CHAPTER SIX

CONCLUSION

6. Conclusion

The adsorption of malachite green onto chitosan was studied in a batch system as a function of temperatures, pH and contact time. The optimum contact time for adsorption of malachite green onto chitosan was found as 6 hours by plotting the amount of malachite green adsorbed (C_s, mg L^{-1}) measured in the certain (definite) time intervals versus time. The shapes of the adsorption isotherms of malachite green on chitosan correspond to L type according to the Giles classification as shown in Fig. 5.5. The L curve indicates that there is no strong competition from the solvent for sites on the surface. Another possibility is that, if the adsorbate has linear or planar molecules, the major axis is parallel to surface. In that study, it can be easily said that chitosan has a medium affinity for the MG molecules. The curves tend to constant value of C_s and reach a plateau showing the formation of a complete monolayer of MG covering adsorbent surface. The amount of MG adsorbed by chitosan is increased by increasing temperature.

Linear form of Langmuir, Freundlich adsorption isotherms is applied to evaluate adsorption data. As can be seen Table 5.2 and 5.3, Langmuir adsorption isotherms gave a better fit than the Freundlich model based on the correlation coefficients (R^2) values. By using Langmuir equation, maximum adsorption capacities (C_m) of chitosan were obtained as 93.55 mgL^{-1} at 30°C, 72.83 mgL^{-1} at 40°C and 82.17 mgL^{-1} at 50°C respectively. Freundlich K_f (adsorption capacity) values from 28.38 mgL^{-1} at 30°C to 76.23 mgL^{-1} at 50°C. As a result, adsorption of malachite green increases by increasing temperatures. Favorable adsorption for malachite green was occurred since the values of R_L (dimensionless separation factor) were between 0-1 and Freundlich n_f heterogeneity factor) values were smaller than1. The values of R_L (Dimensionless separation factor) and n_f values at different temperatures are reported Table 5.2 and 5.3.

The adsorption removal of dye from aqueous solution is pH dependent. The maximum adsorption at adsorption at equilibrium was observed at pH=7.8 by plotting the amount of malachite green adsorbed by chitosan versus equilibrium pH. The interaction between cationic MG and the pair of electrons of nitrogen present in the structure of chitosan occurs. It is clear that the adsorption of dye onto chitosan at basic pH values is high.

Several kinetic models including the pseudo first order equation, pseudo second order equation and intraparticle diffusion model were applied to find out adsorption mechanism. As can be seen from Table 5.6 and 5.9, the correlation coefficients (R_1^2) for pseudo first order kinetic model are between 0.810 and 0.958 and the correlation coefficients (R^2) for kinetic pseudo second order kinetic model are between 0.998 and 1.000. These results show that the adsorption system obeys the pseudo second order kinetic model. If the intraparticle diffusion is involved in the adsorption process, then a plot of the square root of time ($t^{1/2}$) versus uptake (q_t) would results in a linear relationship and the particle diffusion would be the controlling step if this line passed through the origin. When the plots do not pass through the origin, this is indicative of some degree of boundary layer control and the further show that the intraparticle diffusion is not the only rate-controlling step, but also other processes may control the rate of adsorption.

As shown Table 5.15, the values ΔH^0 and ΔS^0 were positive for adsorption of MG onto chitosan. The positive value of ΔH^0 indicates that the adsorption process is endothermic in nature and the positive value ΔS^0 showed the increase in degree of freedom or increases the disorder of adsorption process. Adsorption energy obtained is 85.57 $kJmol^{-1}$ with the correlation coefficient (R) 0.936. This activation energy value is not between 5-40 $kJmol^{-1}$ values. Since it is high, it is understood that the chemical adsorption mechanism is occurred. It can be easily said that the positive value of E_a represents the nature of chemical adsorption of MG onto chitosan; there is an energy barrier in the adsorption process.

Surface Morphology of synthesized chitosan beads can be seen in Figures 5.20, 5.21, 5.22, 5.23 and 5.24 at different magnifications. Pores with different size were observed. Micro-particles are also observed. Some of them are spherical and adhere to each other and held together. The Pores smaller than 1 μm are observed on the surface of the chitosan bead (Figure 5.24).

In the spectra of FTIR of chitosan bead before and after adsorption the wide band at 3430 cm^{-1} shown in the spectrum of chitosan bead is attributed to stretching vibration of hydroxyl group of chitosan. This band was decreased to 3423 cm^{-1} when MG was adsorbed. The bands observed at 1640 cm^{-1} and 1562 cm^{-1} correspond to N-H bending vibrations. These bands increased to 1654 cm^{-1} and 1589 cm^{-1} when the adsorption of MG occurs. These changes may be owing to weak interactions between MG and chitosan. Presumably it can be claimed that hydrogen bonding occurs between nitrogen and hydrogen of chitosan and MG. It was confirmed that adsorption of MG onto chitosan has successfully occurred.

As a conclusion, chitosan can be used as adsorbent for the removal of MG from aqueous solution.

REFERENCES

Aksu,Z., & Kabasakal,E.(2004). *Batch adsorption of 2,4-dichlorophenoxy-acetic acid (2-4-D) from aqueous solution by granular activated carbon. Separation and Purification Technology*, 35, 223-240.

Allen,S. J., Gan, Q., Matthews, R., & Johnson., P.A. (2003). *Comporison of optimized isotherm models for basic dye adsorption by kudzu.Bioresource Technology,* 88, 143-152. Retrieved June 22,2004 from Elsevier database.

Bekçi Z., *Adsorption of Trimethophrim from aqueous solution onto clays*. Dokuz Eylül Üniversitesi, Fen Bilimleri Enstitüsü, İzmir-Turkey, (2005).

Blatt, H., Middleton, G., &Murray, R. (1980). Origin of sedimentary rocks (2d ed.): Englewood Cliffs, N.J., Prentice-Hall, 766 p.

Freundlich, H., 1906. Adsorption in Solution. Phys. Chemie. 57, 384-410.

Gereli, Gürhan. *Adsorption of Promethazine Hydrochloride onto Montmorillonite K10 from aqueous solution*. Dokuz Eylül Üniversitesi, Fen Bilimleri Enstitüsü, İzmir-Turkey. (2005).

Ghiaci,M., Abbaspur, A., Kra, R., & SEYEDEYN, A.F (2004). *Equilibrium isotherm studies fort he sorption of benzene, toluene, and phenol onto orgono-zeolites and as synthesized MCM*, 41, 40, 217-229.

Giles, H., Mc Ewan T. .H.,Nakhwa, S.N., & Smith, D., (1960). *Studies in adsorption Part II. A system of classification of solution adsorption isotherms*. J. Chem. Soc.,4, 3973-3993.

Gordon M. Barrow (1996). Physical Chemistry, US, Mc. Graw Hill Book Comp.

Hiller, S. (1995). *Erosion, sedimentation and sedimentary origin of clays, in Velde,B., ed., Origin and mineralogy of clays*: New York, Springer-Verlag, p. 162-219.

IUPAC Compendium of Chemical Terminology 2nd Edition, 1997.

K. Vasanth Kumar, V. Ramamurthi & S. Sivanesan (2005). *Biosorption of malachite green,* a cationic *dye onto pithophora sp., a fresh water algae*. Department of Chemical Engineering, A. C. Tech, Anna University, Guindy, Chennai-600 025, Tamil Nadu, India.

Mahramanlioğlu, M., Kirbasalar, S.I., & Kizilcikli, I . (2003). *Mass transfer and adsorption kinetics during the adsorption of fluoride onto activated clays in agitated systems*. Fresenius Environmental Bulletin, 12, 1483-1491.

Marcewski, A.W. (2002). *A practical quide to isotherms of adsorption on heterogeneous surfaces.* Retrieved February 1,2004 , from http://www.2002/ adsorption org/awm/ads/Ads.htm.

McKay, G.,Bino, M.J .,& Altemeni, A. (1986). *External mass transfer during the adsorption of various pollutants onto activated carbon.* Water Research, 20(1), 435-442.

M. Mucha, S. Ludwiczak &M. Kawinska (2005). *Kinetics of water sorption by chitosan and its blends with poly(vinyl alcohol).* Faculty of Process and Environmental Engineering, Lodz Technical University, ul. Wolczanska 215, 90-924 Lodz, Poland.

Özcan, A.S., & Özcan, A.(2004).*Adsorption of acid dyes from aqueous solution onto acid-activated bentonite*. Journal of Colloid and Interface Science, 276, 39-46.

Paulino A. T., Simionato, J. I., Garcia, J.C., Nozaki, J., *Characterization of chitosan*

and chitin produced from silkworm chrysalides. Carbohydrate Polymers, 64 (2006) 98–103.

Pham le Dung, Michel Milas, Marguerite Rinaudo & Jacques Desbrieres (1994). *Water soluble derivatives obtained by controlled chemical modifications of chitosan. CERMA V-CNRS, B.P. 53 X. 38041 Grenoble Cedex, France.*

Seki, Yoldaş. *Adsorption of some herbicides onto orgono-clays from aqueous solution.* Dokuz Eylül Üniversitesi, Fen Bilimleri Enstitüsü, İzmir-Turkey. (2002).

Sposito, G. (1981). The Thermodynamics of Soil Solution. New York, Oxford Univ. Pres.

Sposito, G. (1984). Surface Chemistry of Soils. New York:Oxford Univ. Pres.

Tournassat, C., Greneche, J.-M., Tisserand, D.,&, Charlet, L. (2004). *The titration of clay minerals I. Discontinuous back titration technique combined with CEC measurements.* J. Colloid Interface Sci., 273, 224-233.

Weber, T.W., & Chakkravorti, R.K. (1974). *Pore and solid diffusion models for fixed bedadsorbes*.American Institiude of Chemical Engineers Journal, 20,228.

Wikipedia The free Encylopedia (2006).